

Supporting Information

Solvatochromic Investigation of Highly Fluorescent 2-Aminobithiophene Derivatives

Andréanne Bolduc,¹ Yanmei Dong,¹ Amélie Guérin^{1,2} and W.G. Skene^{1,*}

¹Laboratoire de caractérisation photophysique des matériaux conjugués
Département de Chimie
Université de Montréal
CP 6128, Centre-ville
Montreal, QC

²Current address: ENSCBP- École Nationale Supérieure de Chimie, Biologie et de Physique
Institut Polytechnique de Bordeaux
16, avenue Pey Berland
33607 Pessac Cedex

w.skene@umontreal.ca

Table of Contents

Figure S1. ^1H NMR spectra of 4 in acetone- $\text{d}_6/\text{D}_2\text{O}$	5
Figure S2. ^{13}C NMR spectra of 4 in acetone- $\text{d}_6/\text{D}_2\text{O}$	6
Figure S3. ^1H NMR spectra of 5 in acetone- d_6	7
Figure S4. ^{13}C NMR spectra of 5 in acetone- d_6	8
Figure S5. Normalized absorbance (■) and fluorescence (●) of 1 in dichloromethane.....	9
Figure S6. Temperature dependent fluorescence of 1 in tetrahydrofuran from 300 K (purple) to 180 K (black).....	9
Figure S7. Temperature dependent absolute fluorescence quantum yield of 1 in anhydrous and deaerated tetrahydrofuran.....	10
Figure S8. Normalized absorbance (■) and fluorescence (●) of 2 in dichloromethane.....	10
Figure S9. Normalized absorbance of 2 in toluene (■), ether (●), tetrahydrofuran (▲), ethyl acetate (▼), chloroform (◆), dichloromethane (◄), dimethyl formamide (►) acetonitrile (●), dimethyl sulfoxide (★) and ethanol (◆).....	11
Figure S10. Normalized fluorescence of 2 in toluene (■), ether (●), tetrahydrofuran (▲), ethyl acetate (▼), chloroform (◆), dichloromethane (◄), dimethyl formamide (►) acetonitrile (●), dimethyl sulfoxide (★) and ethanol (◆).....	11
Figure S11. Lippert-Mataga plot of 2.....	12
Figure S12. Fluorescence dependence of 2 with $E_T(30)$	12
Figure S13. Temperature dependent fluorescence of 2 in tetrahydrofuran from 300 K (orange) to 180 K (black).....	13
Figure S14. Normalized absorbance (■) and fluorescence (●) of 3 in dichloromethane.....	13
Figure S15. Temperature dependent absorbance of 3 between 273 K (—) and 243 K (—) in tetrahydrofuran.....	14
Figure S16. Normalized absorbance of 3 in toluene (■), ether (●), tetrahydrofuran (▲), ethyl acetate (▼), chloroform (◆), dichloromethane (◄), dimethyl formamide (►) acetonitrile (●), dimethyl sulfoxide (★) and ethanol (◆).....	14
Figure S17. Normalized fluorescence of 3 in toluene (■), ether (●), tetrahydrofuran (▲), ethyl acetate (▼), chloroform (◆), dichloromethane (◄), dimethyl formamide (►) acetonitrile (●), dimethyl sulfoxide (★) and ethanol (◆).....	15
Figure S18. Lippert-Mataga plot of 3.....	15
Figure S19. Fluorescence dependence of 3 with $E_T(30)$	16
Figure S20. Temperature dependent fluorescence of 3 in tetrahydrofuran from 300 K (orange) to 180 K (black).....	16
Figure S21. Temperature dependent absorbance of 3 in tetrahydrofuran going from 273 K (black) to 248 K (brown).....	17
Figure S22. Fluorescence quenching of 3 as a function of nitrothiophene.....	17
Figure S23. Stern-Volmer quenching for 3 as a function of nitrothiophene.....	18
Figure S24. Fluorescence quenching of 3 as a function of nitromethane.....	18
Figure S25. Stern-Volmer quenching of 3 as a function of nitromethane.....	19
Figure S26. Fluorescence quenching of 3 as a function of methanol.....	19
Figure S27. Fluorescence quenching of 3 as a function of deuterated methanol.....	20
Figure S28. Fluorescence quenching of 3 as a function of isopropanol.....	20
Figure S29. Dynamic Stern-Volmer quenching of 3 as a function of methanol.....	21
Figure S30. Dynamic Stern-Volmer quenching of 3 as a function of deuterated methanol.....	21
Figure S31. Dynamic Stern-Volmer quenching of 3 as a function of isopropanol.....	22
Figure S32. Normalized absorbance (■) and fluorescence (●) of 4 in dichloromethane.....	23

Figure S33. Temperature dependent absorbance of 4 between 273 K (—) and 243 K (—) in tetrahydrofuran.	23
Figure S34. Normalized absorbance of 4 in toluene (■), ether (●), tetrahydrofuran (▲), ethyl acetate (▼), chloroform (◆), dichloromethane (◄), dimethyl formamide (►) acetonitrile (●), dimethyl sulfoxide (★) and ethanol (◆).	24
Figure S35. Normalized fluorescence of 4 in toluene (■), ether (●), tetrahydrofuran (▲), ethyl acetate (▼), chloroform (◆), dichloromethane (◄), dimethyl formamide (►) acetonitrile (●), dimethyl sulfoxide (★) and ethanol (◆).	24
Figure S36. Lippert-Mataga plot of 4.	25
Figure S37. Fluorescence dependence of 4 with $E_T(30)$	25
Figure S38. Temperature dependent fluorescence 4 in tetrahydrofuran from 300 K (orange) to 180 K (black).	26
Figure S39. Temperature dependent absorbance of 4 in tetrahydrofuran between 273 K (black) to 243 K (navy).	26
Figure S40. Cryofluorescence of 4 in anhydrous ethanol between 180 K (—) and 300 K (—).	27
Figure S41. Normalized absorbance (■) and fluorescence (●) of 5 in dichloromethane.	28
Figure S42. Temperature dependent absorbance of 5 between 273 K (—) and 243 K (—) in tetrahydrofuran.	28
Figure S43. Normalized absorbance of 5 in toluene (■), ether (●), tetrahydrofuran (▲), ethyl acetate (▼), chloroform (◆), dichloromethane (◄), dimethyl formamide (►) acetonitrile (●), dimethyl sulfoxide (★) and ethanol (◆).	29
Figure S44. Normalized fluorescence of 5 in toluene (■), ether (●), tetrahydrofuran (▲), ethyl acetate (▼), chloroform (◆), dichloromethane (◄), dimethyl formamide (►) acetonitrile (●), dimethyl sulfoxide (★) and ethanol (◆).	29
Figure S45. Lippert-Mataga plot of 5.	30
Figure S46. Fluorescence dependence of 5 with $E_T(30)$	30
Figure S47. Temperature dependent absolute fluorescence quantum yield of 5 in anhydrous and deaerated tetrahydrofuran.	31
Figure S48. Temperature dependent absorbance of 5 in tetrahydrofuran from 273 K (black) to 245 K (navy).	31
Figure S49. Normalized absorbance (■) and fluorescence (●) of 6 in dichloromethane.	32
Figure S50. Normalized absorbance of 6 in toluene (■), ether (●), tetrahydrofuran (▲), ethyl acetate (▼), chloroform (◆), dichloromethane (◄), dimethyl formamide (►) acetonitrile (●), dimethyl sulfoxide (★) and ethanol (◆).	32
Figure S51. Normalized fluorescence of 6 in toluene (■), ether (●), tetrahydrofuran (▲), ethyl acetate (▼), chloroform (◆), dichloromethane (◄), dimethyl formamide (►) acetonitrile (●), dimethyl sulfoxide (★) and ethanol (◆).	33
Figure S52. Lippert-Mataga plot of 6.	33
Figure S53. Fluorescence dependence of 6 with $E_T(30)$	34
Figure S54. Temperature dependent fluorescence of 6 in tetrahydrofuran from 300 K (orange) to 180 K (black).	34
Figure S 55. Solvatochromism of 2,3 and 6 under ambient light (left) and UV light (right)...	35
Figure S56. Quenching kinetics of 1 with 1,3-cyclohexadiene in acetonitrile. Inset: transient kinetics of 1 monitored at 420 nm as a function of 1,3-cyclohexadiene.	35
Figure S57. Quenching kinetics of 1 with 2-methylnaphthalene in acetonitrile. Inset: transient kinetics of 1 monitored at 420 nm as a function of 2-methylnaphthalene.	36
Figure S58. Quenching kinetics of 2 with 1,3-cyclohexadiene in acetonitrile. Inset: transient kinetics of 2 monitored at 420 nm as a function of 1,3-cyclohexadiene.	36

Figure S59. Quenching kinetics of 2 with 2-methylnaphthalene in acetonitrile. Inset: transient kinetics of 2 monitored at 420 nm as a function of 2-methylnaphthalene.	37
Figure S60. Transient absorbance spectra of 3 in acetonitrile upon excited at 355 nm.	37
Figure S61. Transient absorbance kinetic of 3 monitored at 650 nm in acetonitrile.	38
Figure S62. Transient absorbance spectra of 4 in acetonitrile upon excited at 355 nm.	38
Figure S63. Transient absorbance kinetic of 4 monitored at 550 nm in acetonitrile.	39
Figure S64. Transient absorbance spectra of 5 in acetonitrile upon exciting at 355 nm.	39
Figure S65. Transient absorbance kinetic of 5 monitored at 550 nm in acetonitrile.	40
Figure S66. Cyclic voltammograms showing the anodic processes of 1 (—), 2 (—), 3 (—), 4 (—), 5 (—) and 6 (—) in deaerated dichloromethane with 0.1 M TBAPF ₆ at 100 mV s ⁻¹ with ferrocene as an internal reference (E _{pa} = 435 mV vs. SCE).	42
Figure S67. Cathodic cyclic voltammogram of 2 in dichloromethane with 0.1 M TBAPF ₆ at 100 mVs ⁻¹	42
Figure S68. Cathodic cyclic voltammogram of 3 in dichloromethane with 0.1 M TBAPF ₆ at 100 mVs ⁻¹	43
Figure S69. Cathodic cyclic voltammogram of 4 in dichloromethane with 0.1 M TBAPF ₆ at 100 mVs ⁻¹	43
Figure S70. Cathodic cyclic voltammogram of 5 in dichloromethane with 0.1 M TBAPF ₆ at 100 mVs ⁻¹	44
Figure S71. Cathodic cyclic voltammogram of 6 in dichloromethane with 0.1 M TBAPF ₆ at 100 mVs ⁻¹	44

^1H NMR and ^{13}C NMR Spectra.

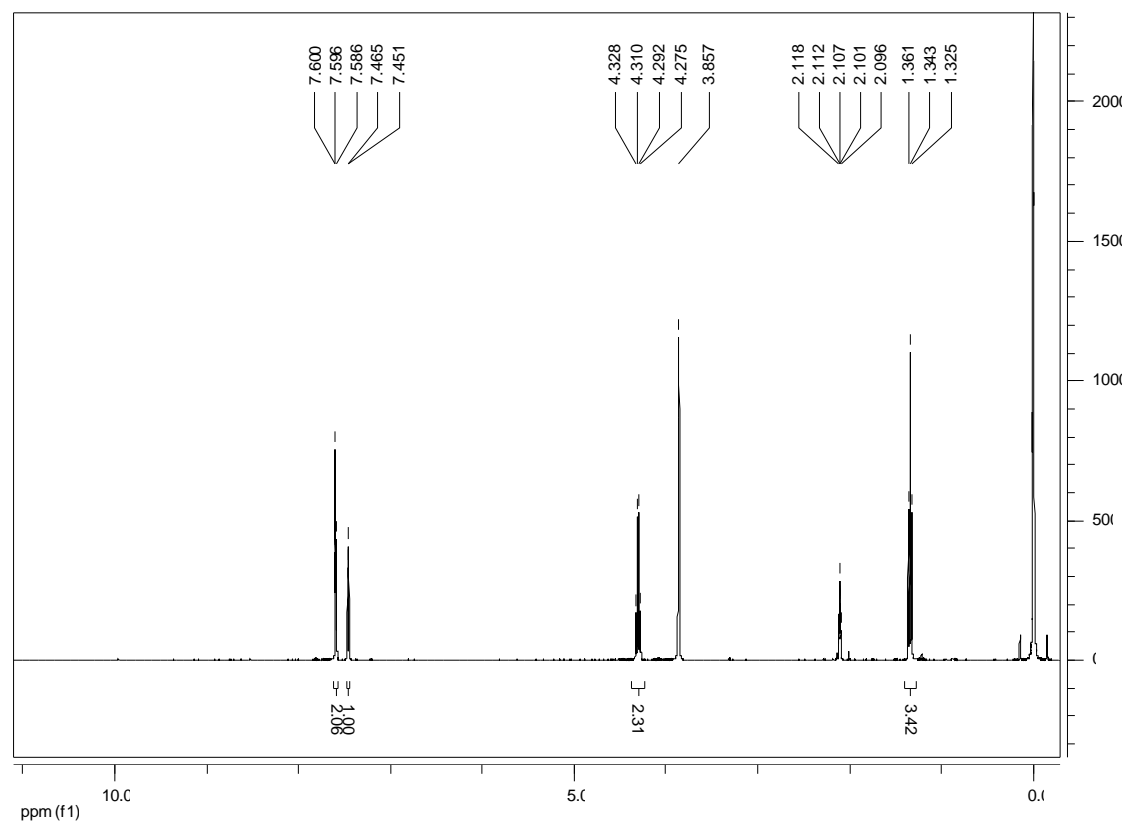


Figure S1. ^1H NMR spectra of 4 in acetone- d_6 /D $_2$ O

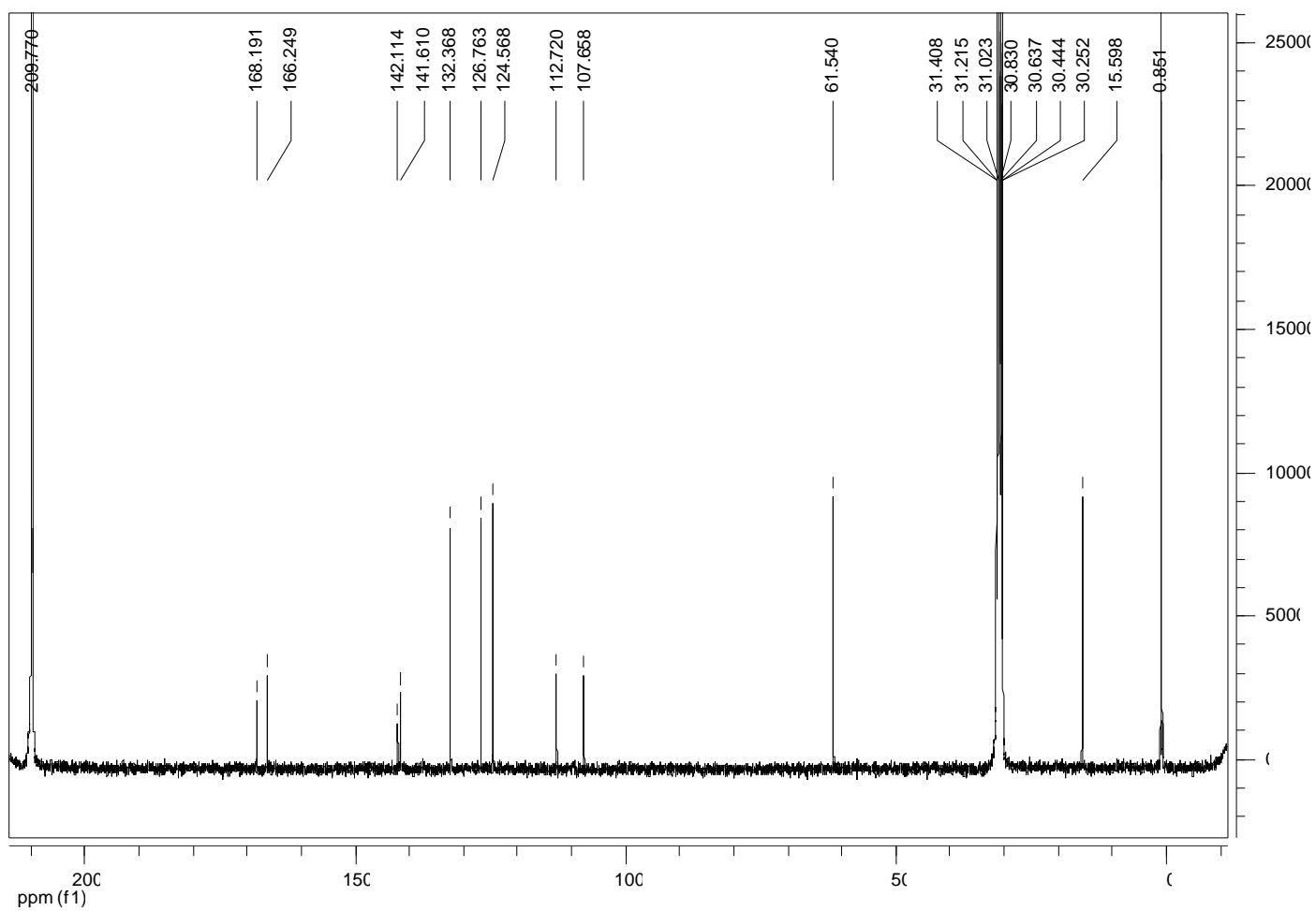


Figure S2. ^{13}C NMR spectra of **4** in acetone- d_6 / D_2O

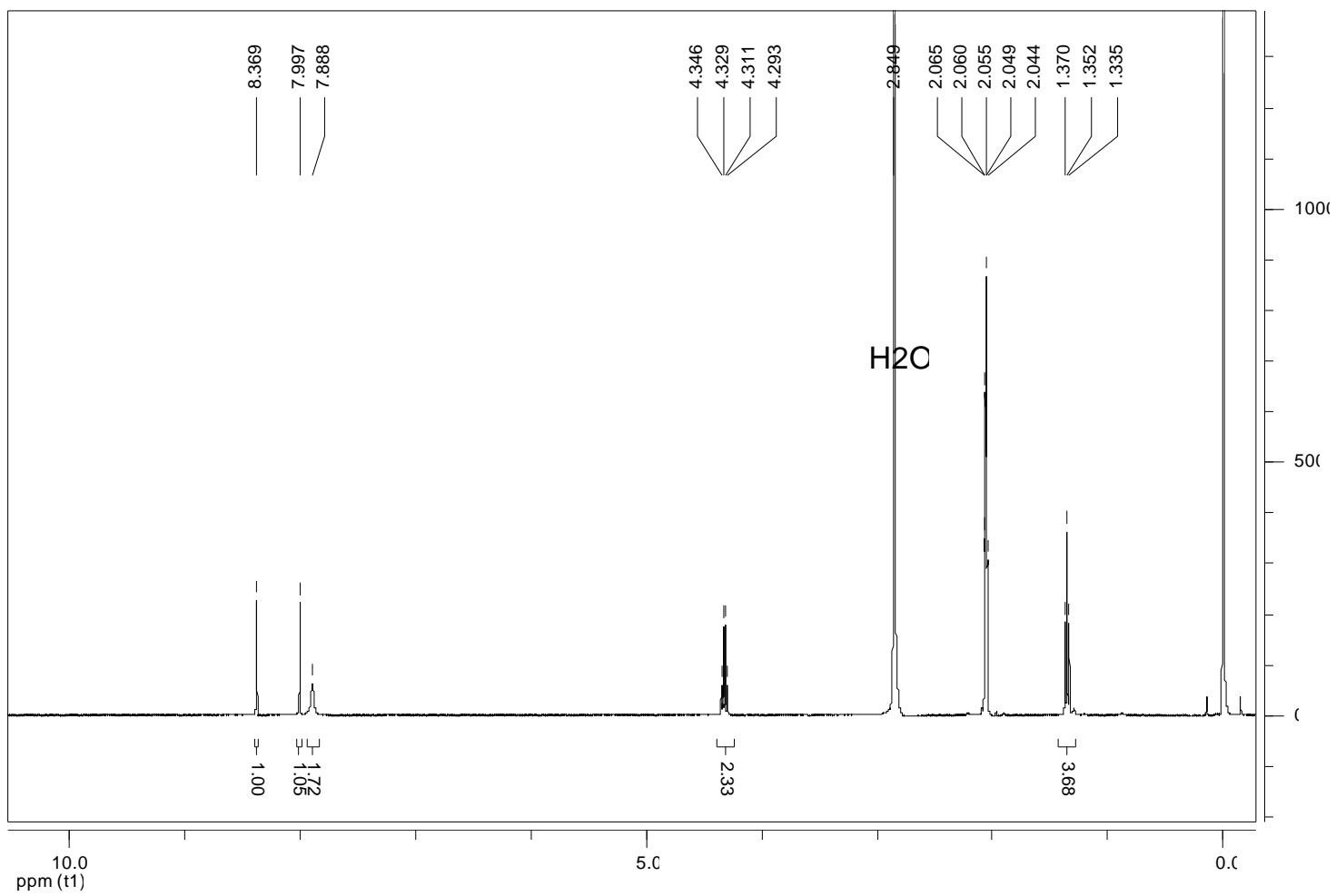


Figure S3. ^1H NMR spectra of **5** in acetone- d_6

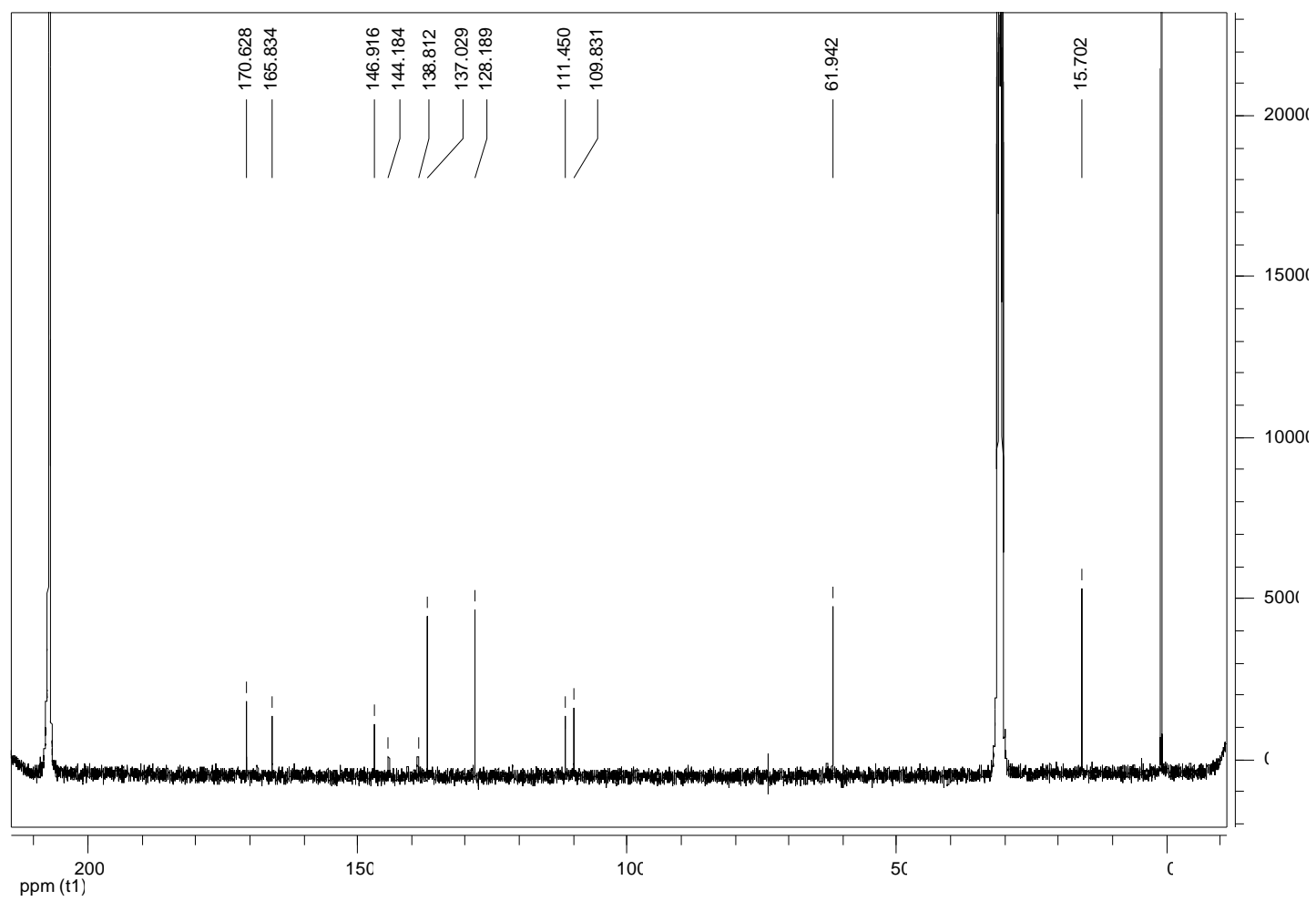


Figure S4. ^{13}C NMR spectra of **5** in acetone- d_6

Photophysical Properties

Photophysical properties of **1**.

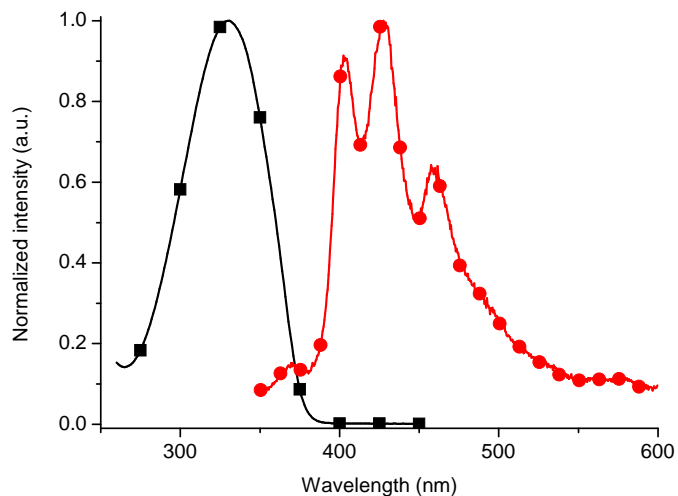


Figure S5. Normalized absorbance (■) and fluorescence (●) of **1** in dichloromethane.

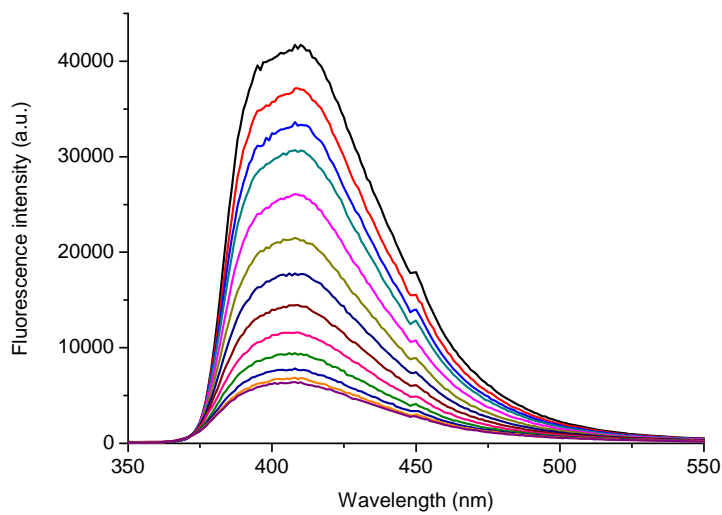


Figure S6. Temperature dependent fluorescence of **1** in tetrahydrofuran from 300 K (**purple**) to 180 K (**black**).

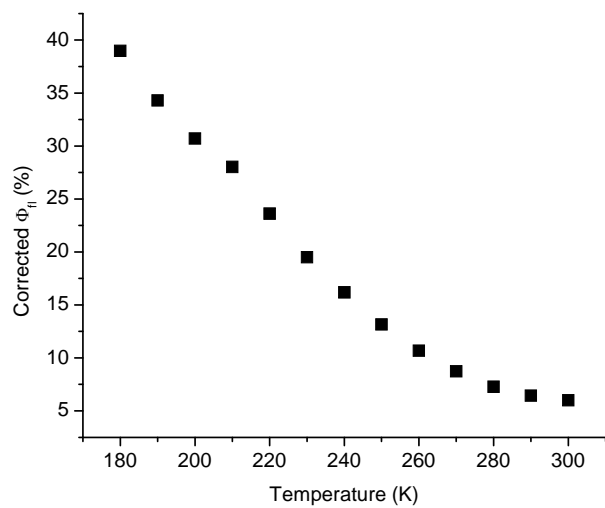


Figure S7. Temperature dependent absolute fluorescence quantum yield of **1** in anhydrous and deaerated tetrahydrofuran.

Photophysical properties of **2**.

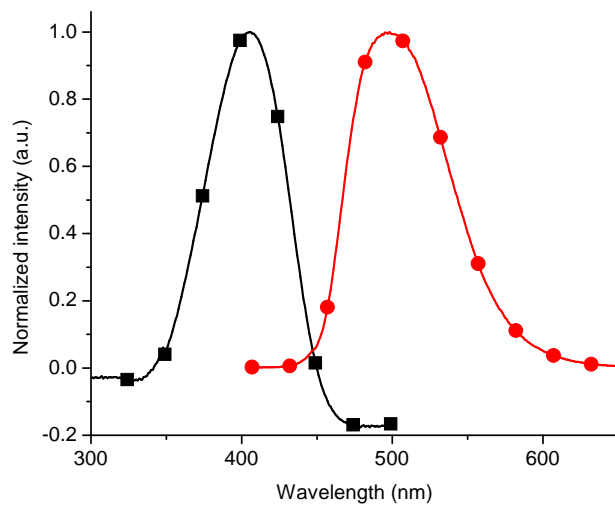


Figure S8. Normalized absorbance (■) and fluorescence (●) of **2** in dichloromethane.

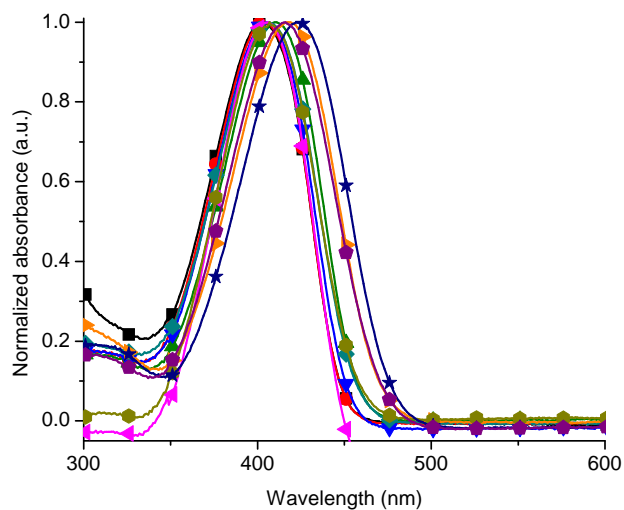


Figure S9. Normalized absorbance of **2** in toluene (■), ether (●), tetrahydrofuran (▲), ethyl acetate (▼), chloroform (◆), dichloromethane (◄), dimethyl formamide (►) acetonitrile (◆), dimethyl sulfoxide (★) and ethanol (◆).

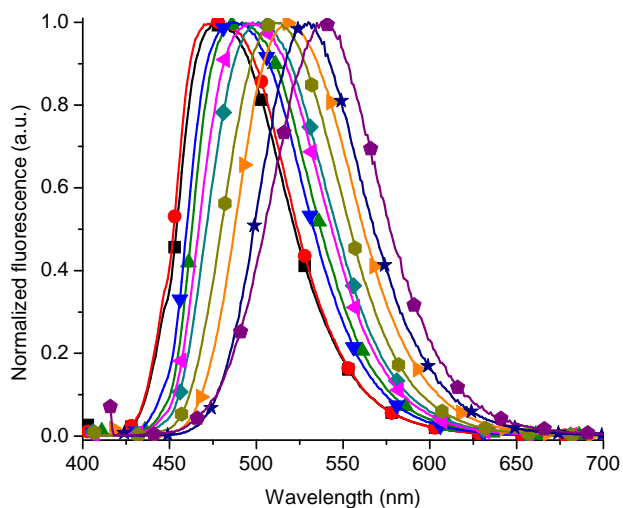


Figure S10. Normalized fluorescence of **2** in toluene (■), ether (●), tetrahydrofuran (▲), ethyl acetate (▼), chloroform (◆), dichloromethane (◄), dimethyl formamide (►) acetonitrile (◆), dimethyl sulfoxide (★) and ethanol (◆).

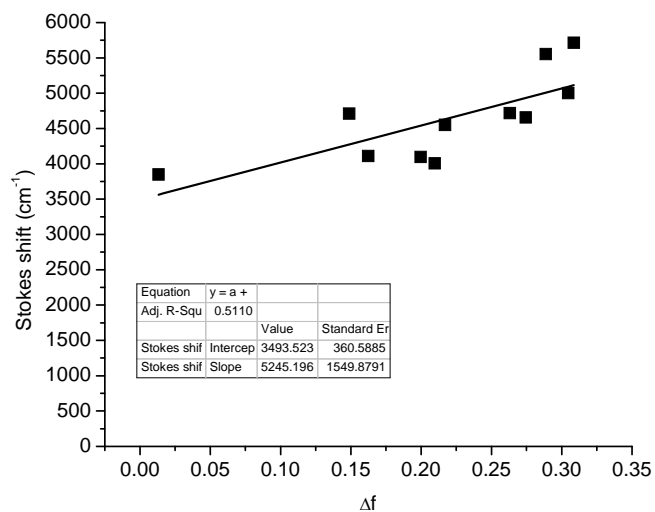


Figure S11. Lippert-Mataga plot of **2**.

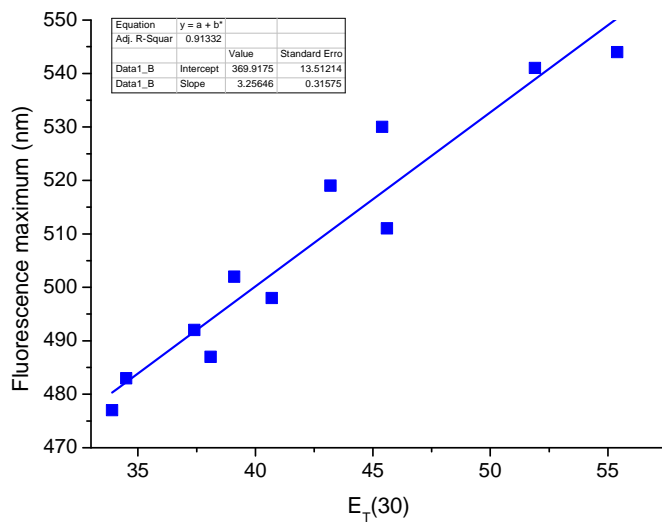


Figure S12. Fluorescence dependence of **2** with $E_T(30)$.

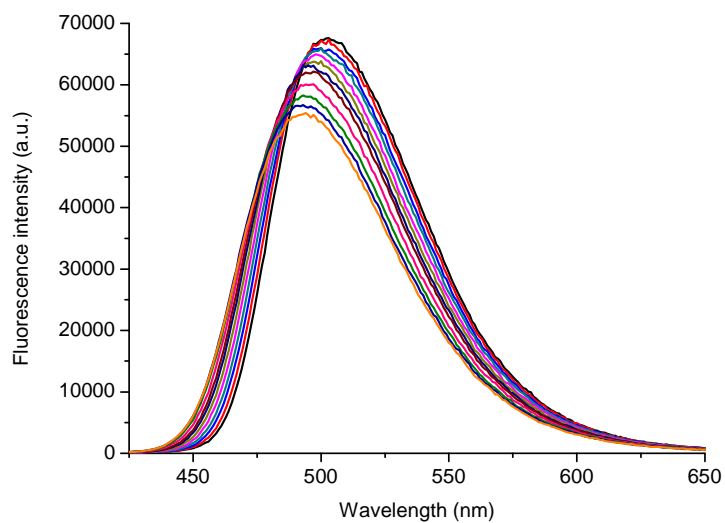


Figure S13. Temperature dependent fluorescence of **2** in tetrahydrofuran from 300 K (orange) to 180 K (black).

Photophysical properties of **3**.

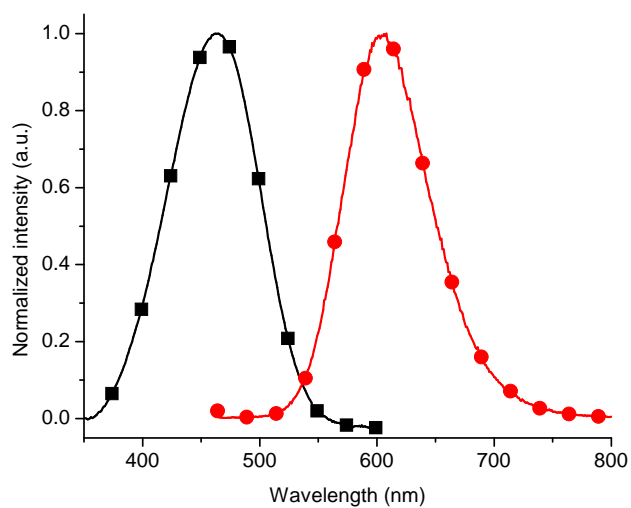


Figure S14. Normalized absorbance (■) and fluorescence (●) of **3** in dichloromethane.

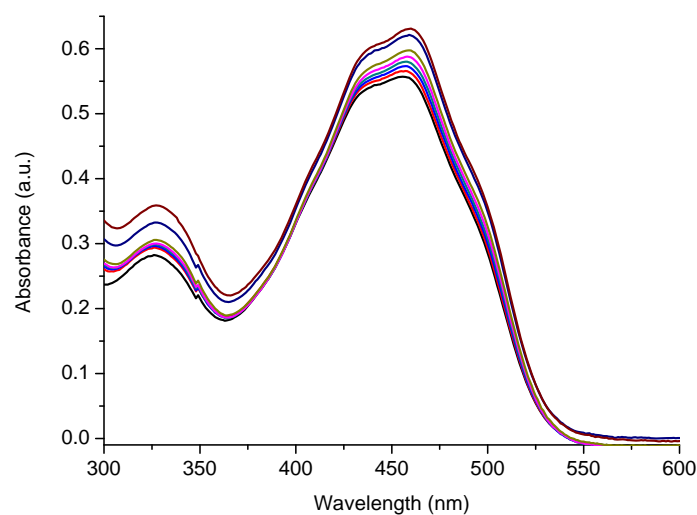


Figure S15. Temperature dependent absorbance of **3** between 273 K (—) and 243 K (—) in tetrahydrofuran.

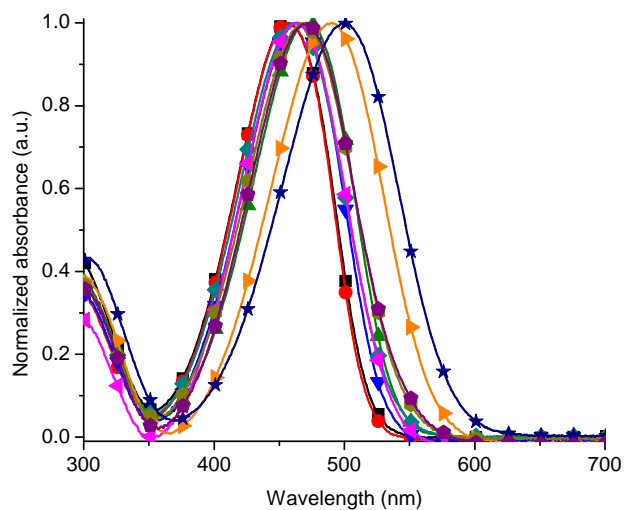


Figure S16. Normalized absorbance of **3** in toluene (■), ether (●), tetrahydrofuran (▲), ethyl acetate (▼), chloroform (◆), dichloromethane (◀), dimethyl formamide (▶) acetonitrile (◇), dimethyl sulfoxide (★) and ethanol (◆).

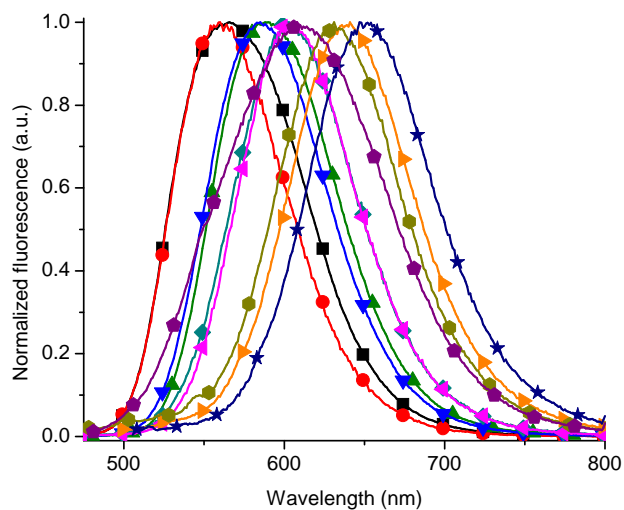


Figure S17. Normalized fluorescence of **3** in toluene (■), ether (●), tetrahydrofuran (▲), ethyl acetate (▼), chloroform (◆), dichloromethane (◀), dimethyl formamide (▶) acetonitrile (●), dimethyl sulfoxide (★) and ethanol (◆).

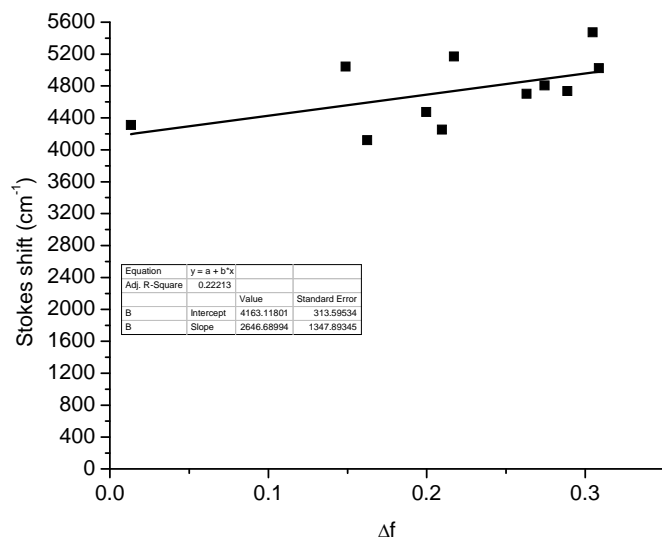


Figure S18. Lippert-Mataga plot of **3**.

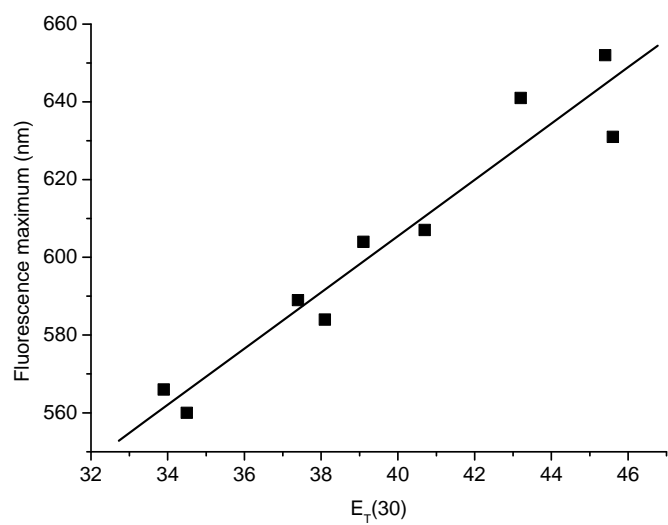


Figure S19. Fluorescence dependence of **3** with $E_T(30)$.

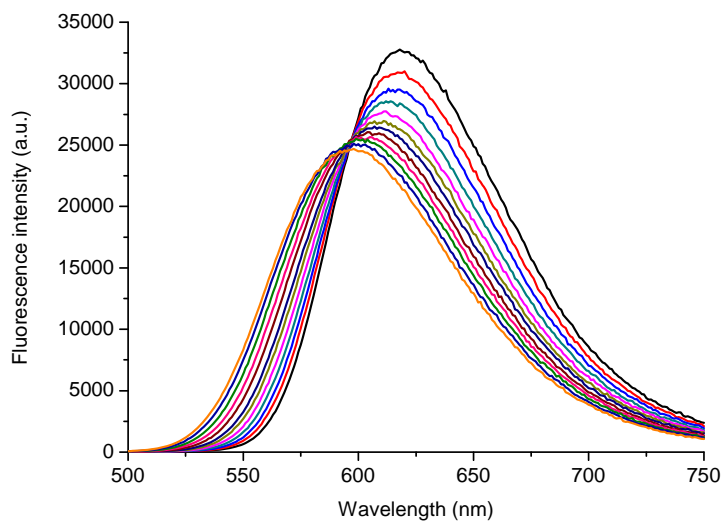


Figure S20. Temperature dependent fluorescence of **3** in tetrahydrofuran from 300 K (**orange**) to 180 K (**black**).

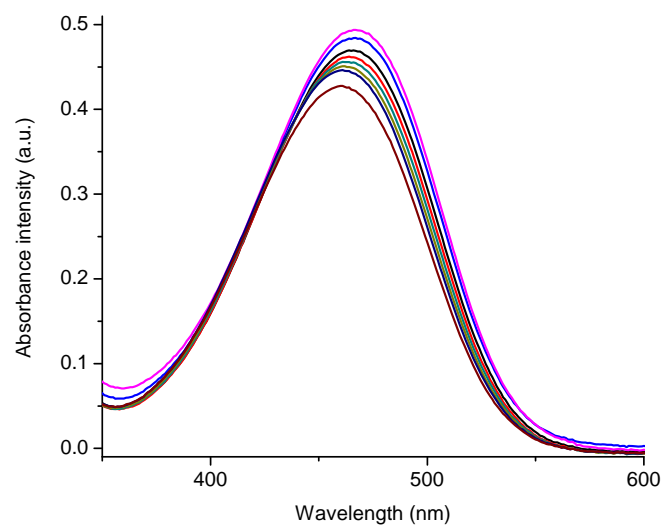


Figure S21. Temperature dependent absorbance of **3** in tetrahydrofuran going from 273 K (black) to 248 K (brown).

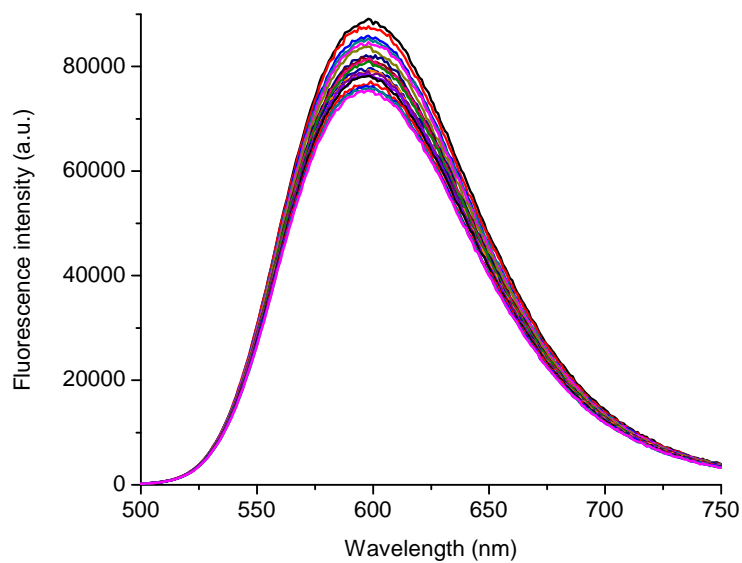


Figure S22. Fluorescence quenching of **3** as a function of nitrothiophene.

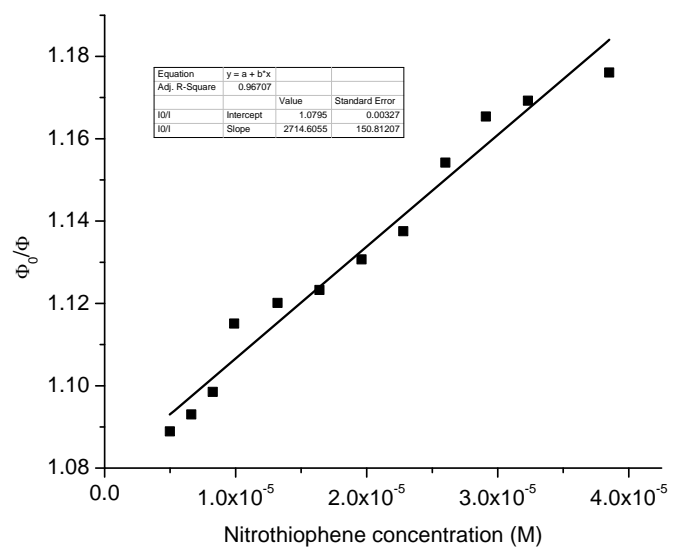


Figure S23. Stern-Volmer quenching for **3** as a function of nitrothiophene.

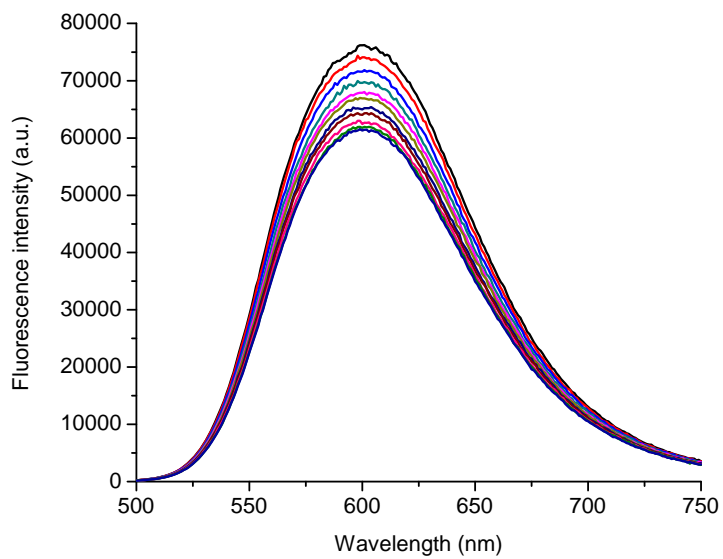


Figure S24. Fluorescence quenching of **3** as a function of nitromethane.

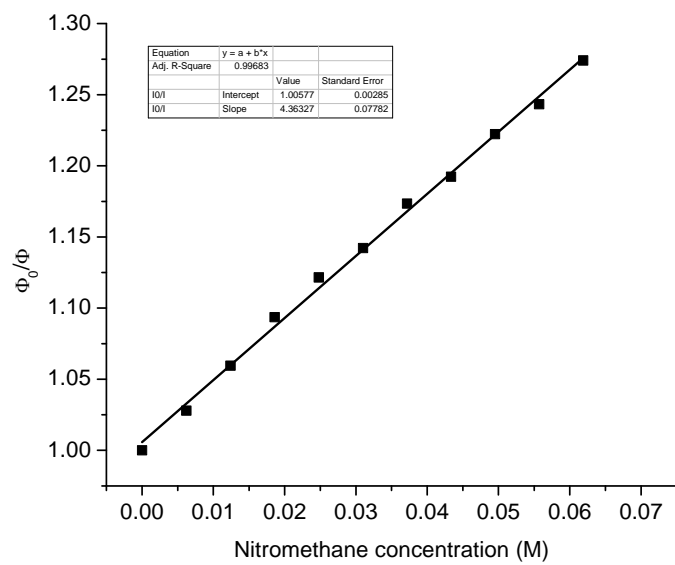


Figure S25. Stern-Volmer quenching of **3** as a function of nitromethane.

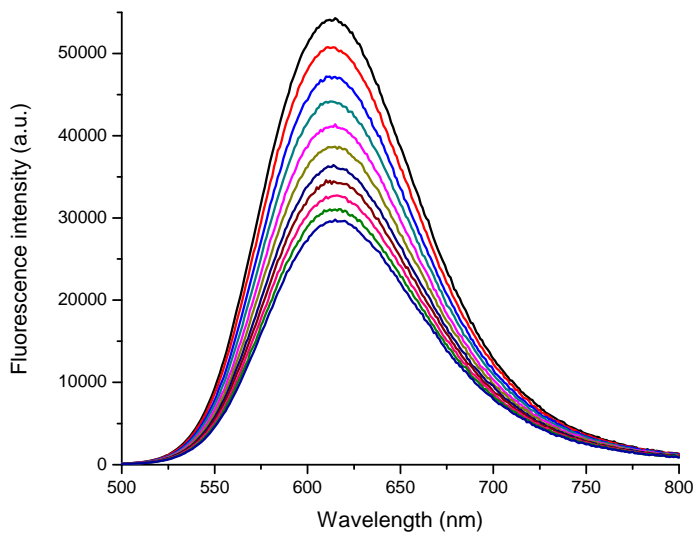


Figure S26. Fluorescence quenching of **3** as a function of methanol.

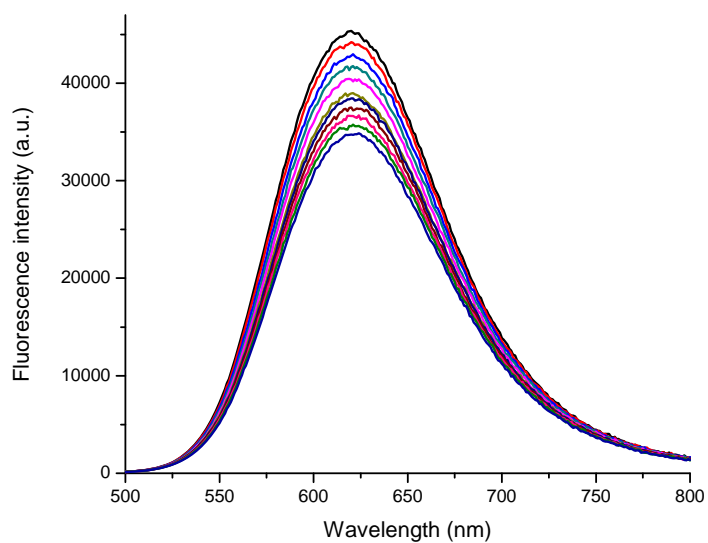


Figure S27. Fluorescence quenching of **3** as a function of deuterated methanol.

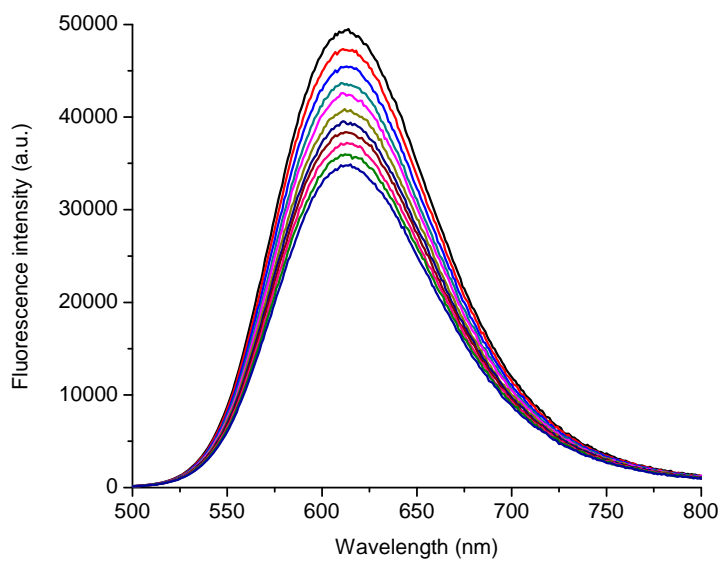


Figure S28. Fluorescence quenching of **3** as a function of isopropanol.

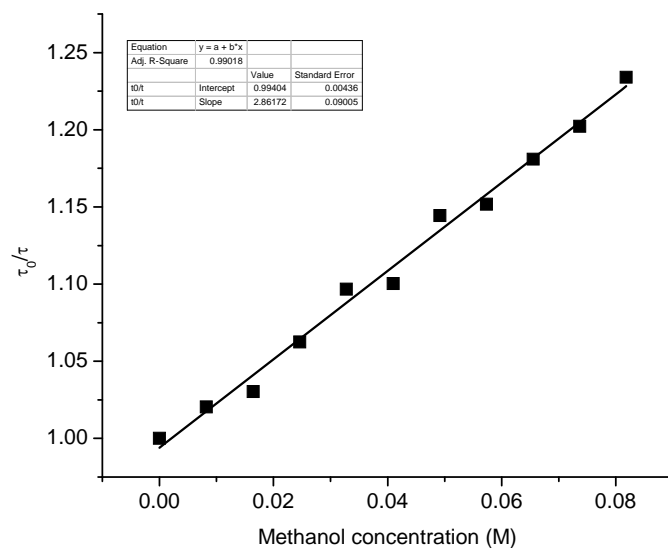


Figure S29. Dynamic Stern-Volmer quenching of **3** as a function of methanol.

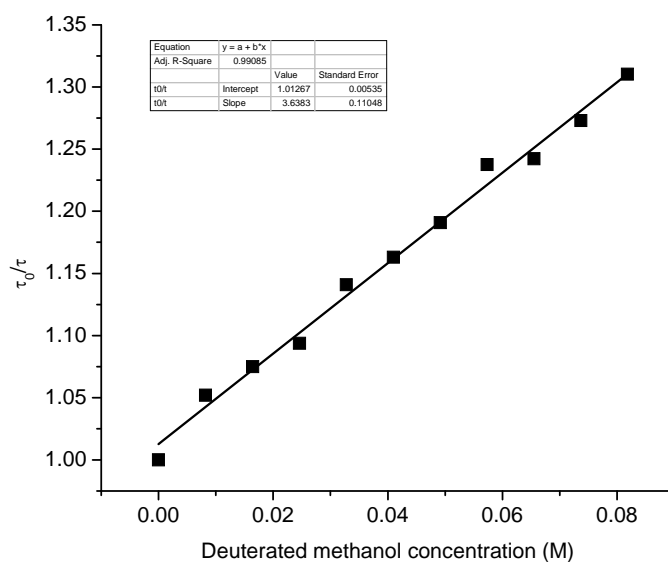


Figure S30. Dynamic Stern-Volmer quenching of **3** as a function of deuterated methanol.

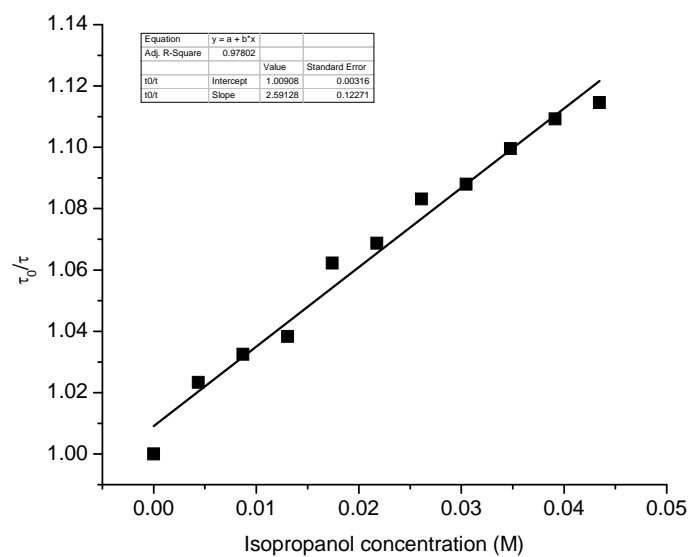


Figure S31. Dynamic Stern-Volmer quenching of **3** as a function of isopropanol.

Photophysical properties of 4

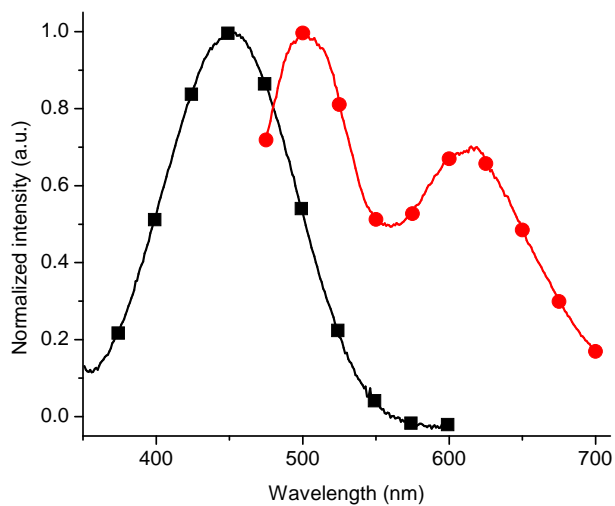


Figure S32. Normalized absorbance (■) and fluorescence (●) of 4 in dichloromethane.

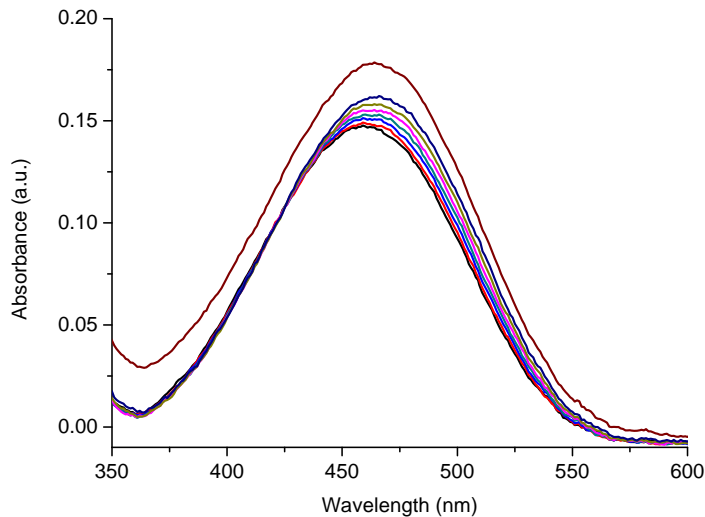


Figure S33. Temperature dependent absorbance of 4 between 273 K (—) and 243 K (—) in tetrahydrofuran.

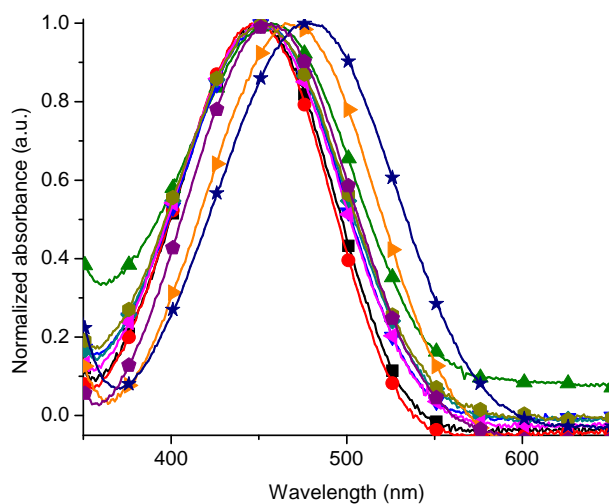


Figure S34. Normalized absorbance of **4** in toluene (■), ether (●), tetrahydrofuran (▲), ethyl acetate (▼), chloroform (◆), dichloromethane (◄), dimethyl formamide (►) acetonitrile (◇), dimethyl sulfoxide (★) and ethanol (◆).

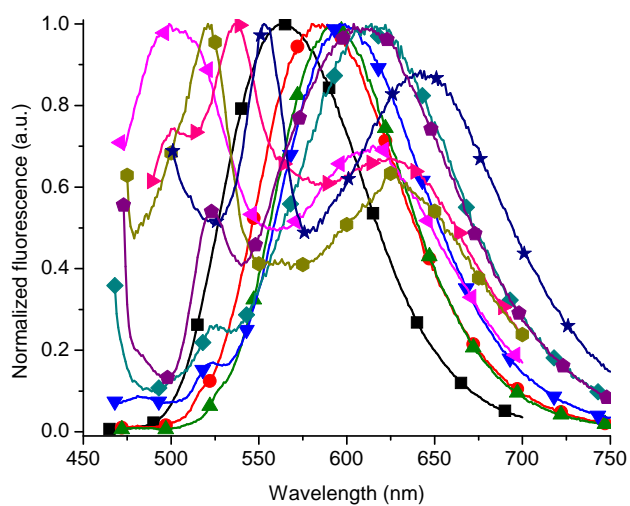


Figure S35. Normalized fluorescence of **4** in toluene (■), ether (●), tetrahydrofuran (▲), ethyl acetate (▼), chloroform (◆), dichloromethane (◄), dimethyl formamide (►) acetonitrile (◇), dimethyl sulfoxide (★) and ethanol (◆).

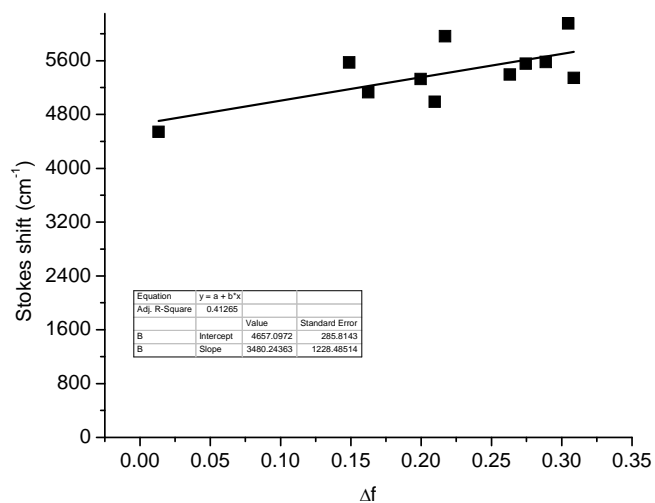


Figure S36. Lippert-Mataga plot of **4**.

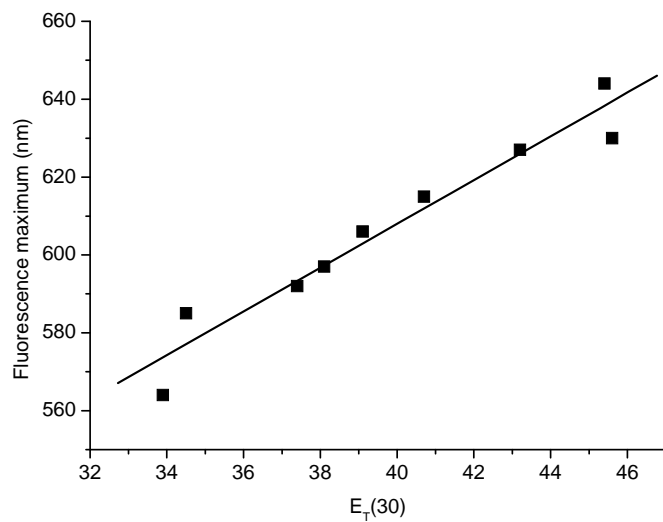


Figure S37. Fluorescence dependence of **4** with E_T(30).

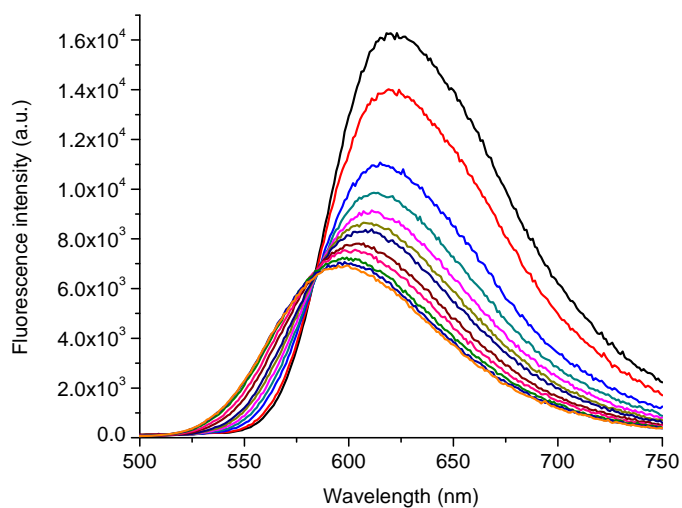


Figure S38. Temperature dependent fluorescence **4** in tetrahydrofuran from 300 K (**orange**) to 180 K (**black**).

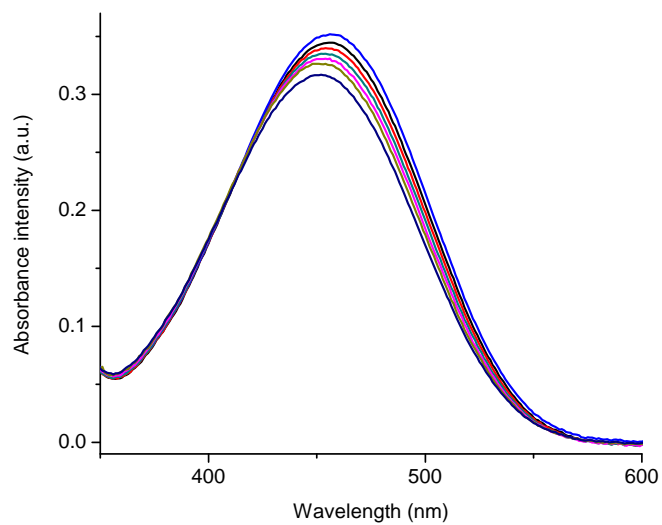


Figure S39. Temperature dependent absorbance of **4** in tetrahydrofuran between 273 K (black) to 243 K (navy).

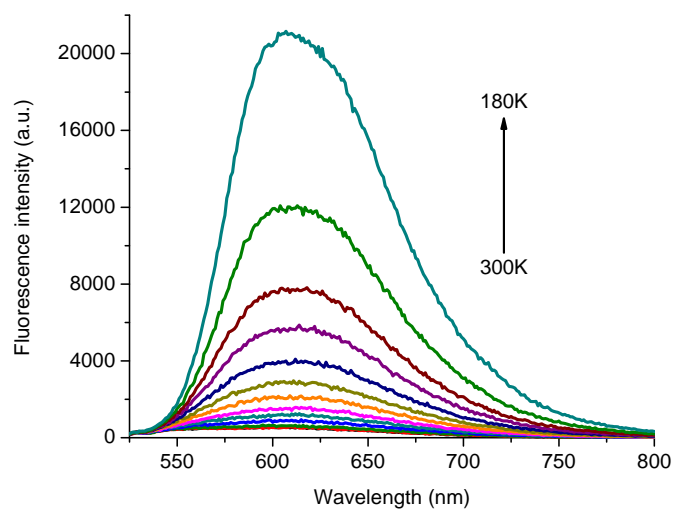


Figure S40. Cryofluorescence of **4** in anhydrous ethanol between 180 K (—) and 300 K (—).

Photophysical properties of **5**.

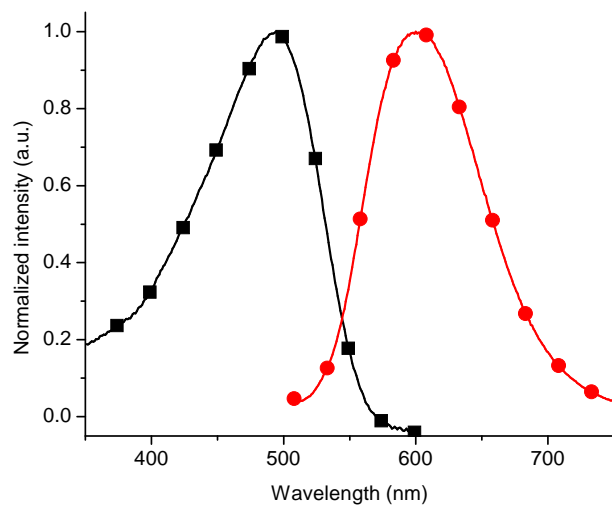


Figure S41. Normalized absorbance (■) and fluorescence (●) of **5** in dichloromethane.

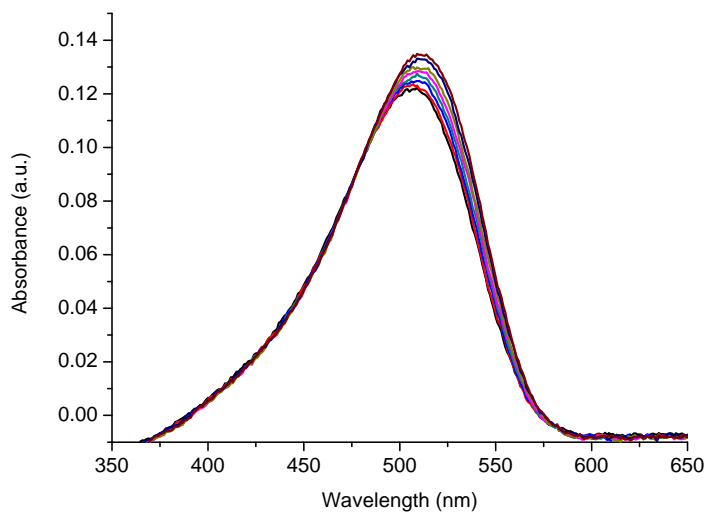


Figure S42. Temperature dependent absorbance of **5** between 273 K (—) and 243 K (—) in tetrahydrofuran.

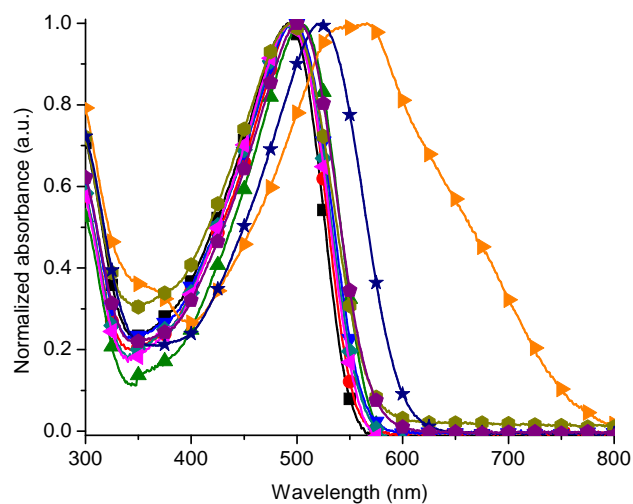


Figure S43. Normalized absorbance of **5** in toluene (■), ether (●), tetrahydrofuran (▲), ethyl acetate (▼), chloroform (◆), dichloromethane (◄), dimethyl formamide (►) acetonitrile (◇), dimethyl sulfoxide (★) and ethanol (◆).

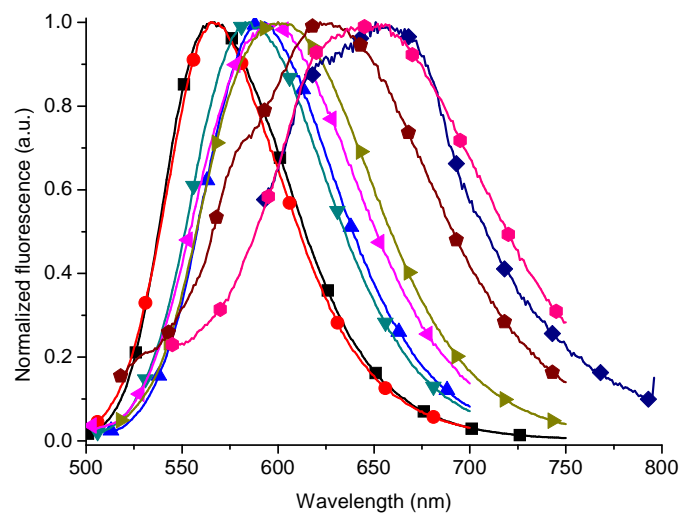


Figure S44. Normalized fluorescence of **5** in toluene (■), ether (●), tetrahydrofuran (▲), ethyl acetate (▼), chloroform (◆), dichloromethane (◄), dimethyl formamide (►) acetonitrile (◇), dimethyl sulfoxide (★) and ethanol (◆).

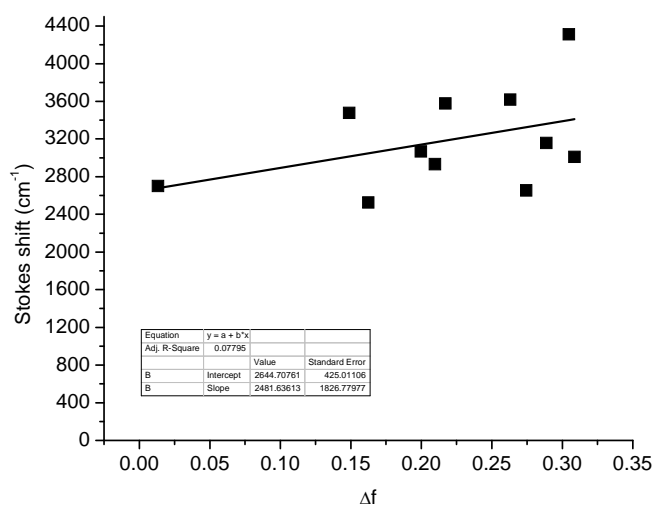


Figure S45. Lippert-Mataga plot of **5**.

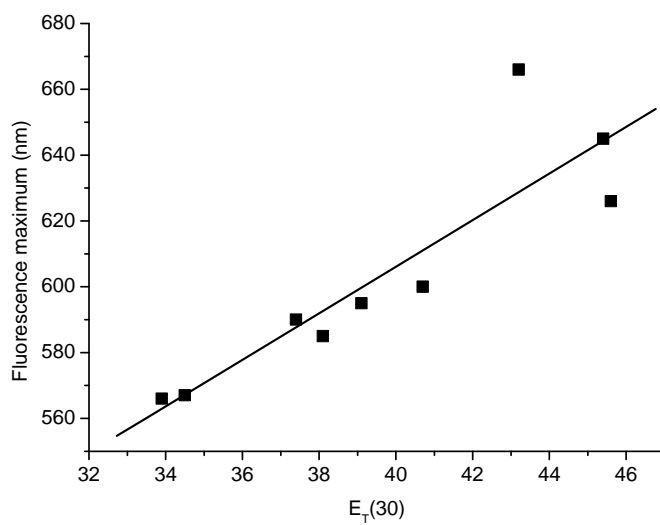


Figure S46. Fluorescence dependence of **5** with E_T(30).

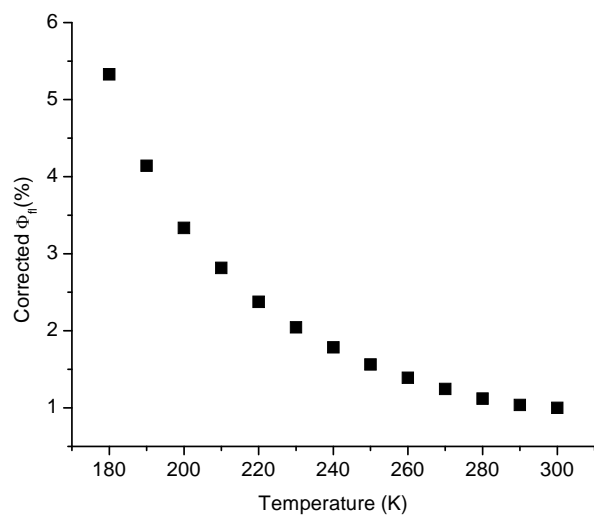


Figure S47. Temperature dependent absolute fluorescence quantum yield of **5** in anhydrous and deaerated tetrahydrofuran.

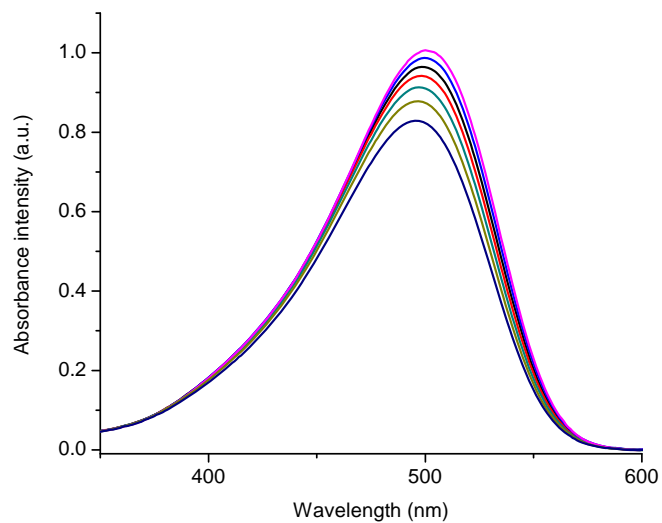


Figure S48. Temperature dependent absorbance of **5** in tetrahydrofuran from 273 K (black) to 245 K (navy).

Photophysical properties of **6**.

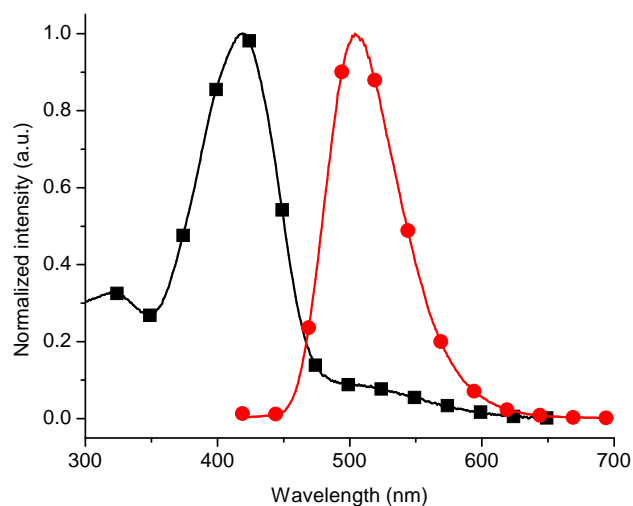


Figure S49. Normalized absorbance (■) and fluorescence (●) of **6** in dichloromethane.

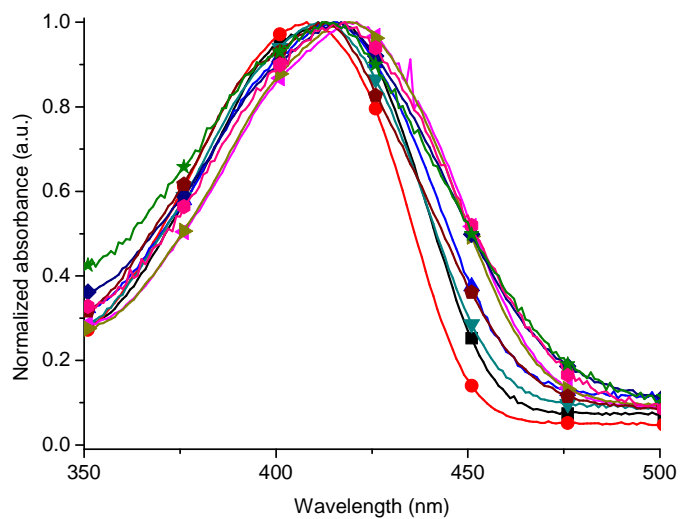


Figure S50. Normalized absorbance of **6** in toluene (■), ether (●), tetrahydrofuran (▲), ethyl acetate (▼), chloroform (◆), dichloromethane (◀), dimethyl formamide (▶), acetonitrile (◆), dimethyl sulfoxide (★) and ethanol (◆).

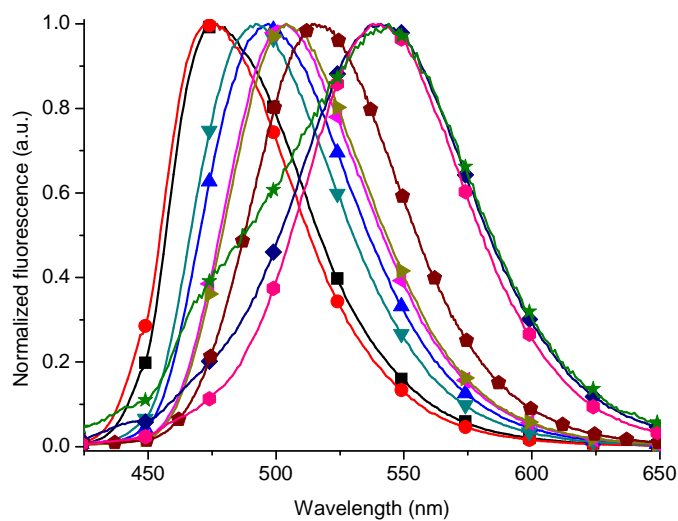


Figure S51. Normalized fluorescence of **6** in toluene (■), ether (●), tetrahydrofuran (▲), ethyl acetate (▼), chloroform (◆), dichloromethane (◀), dimethyl formamide (▶) acetonitrile (◇), dimethyl sulfoxide (★) and ethanol (◆).

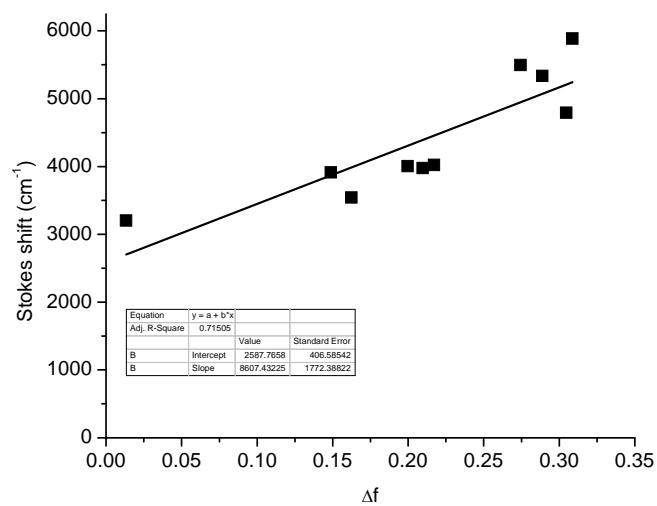


Figure S52. Lippert-Mataga plot of **6**.

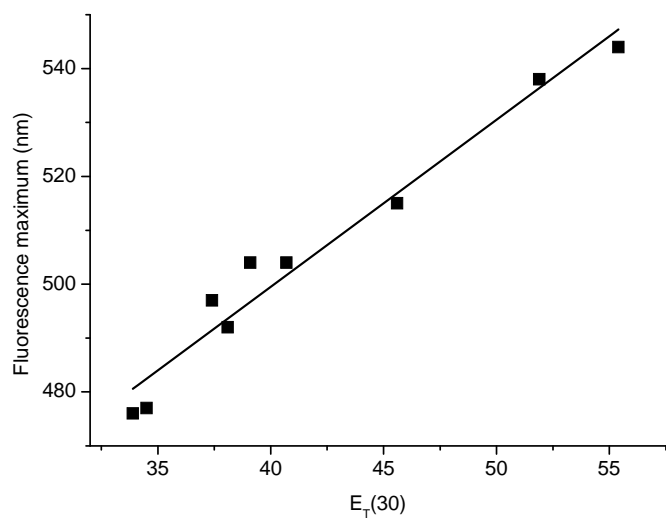


Figure S53. Fluorescence dependence of **6** with $E_T(30)$.

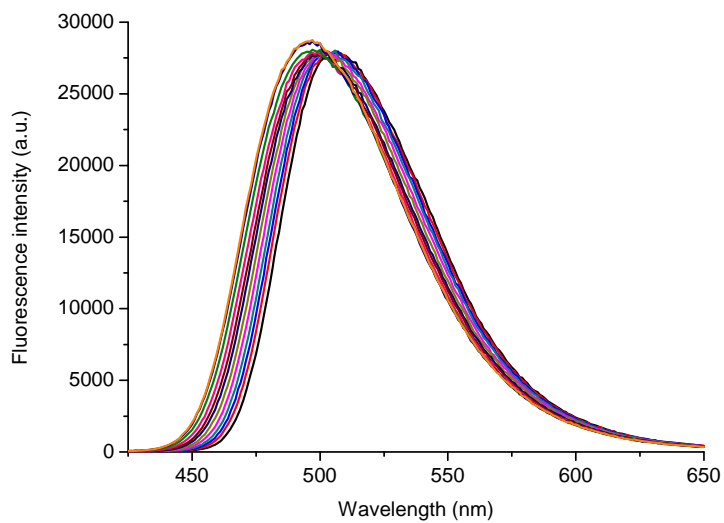


Figure S54. Temperature dependent fluorescence of **6** in tetrahydrofuran from 300 K (orange) to 180 K (black).

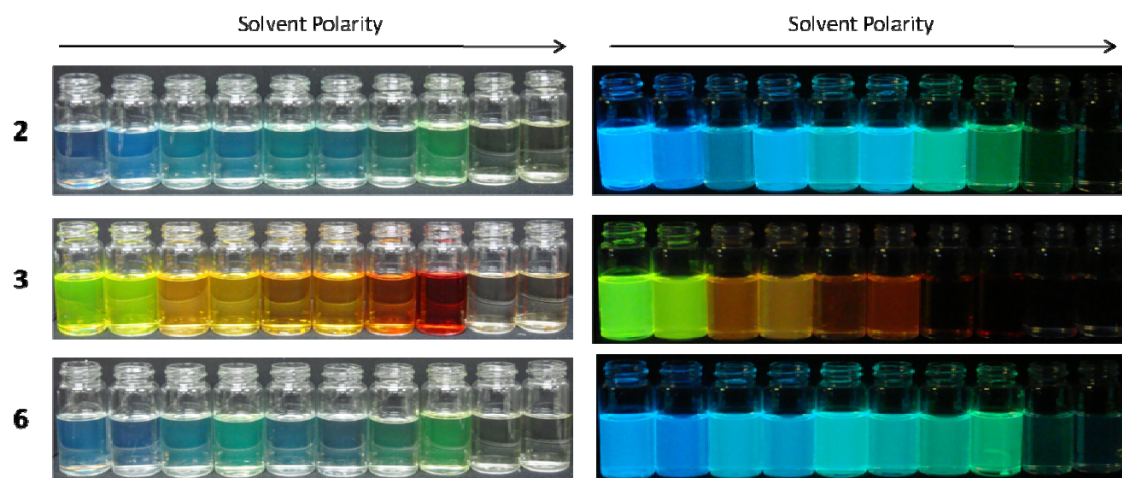


Figure S 55. Solvatochromism of **2**, **3** and **6** under ambient light (left) and UV light (right).

Laser flash photolysis

Laser flash photolysis of **1**

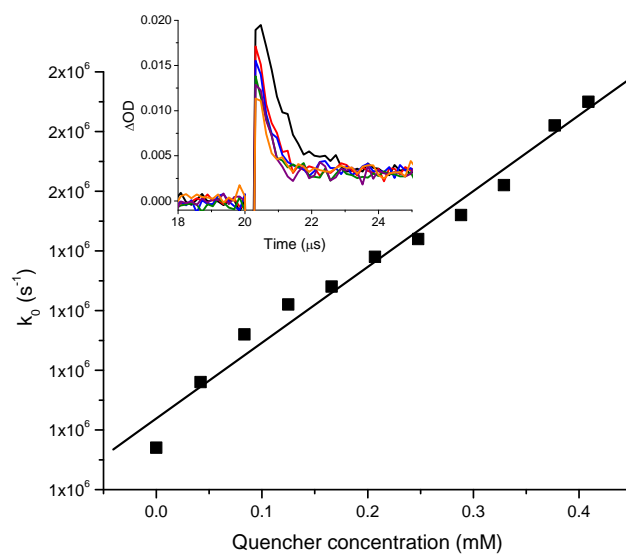


Figure S56. Quenching kinetics of **1** with 1,3-cyclohexadiene in acetonitrile. Inset: transient kinetics of **1** monitored at 420 nm as a function of 1,3-cyclohexadiene.

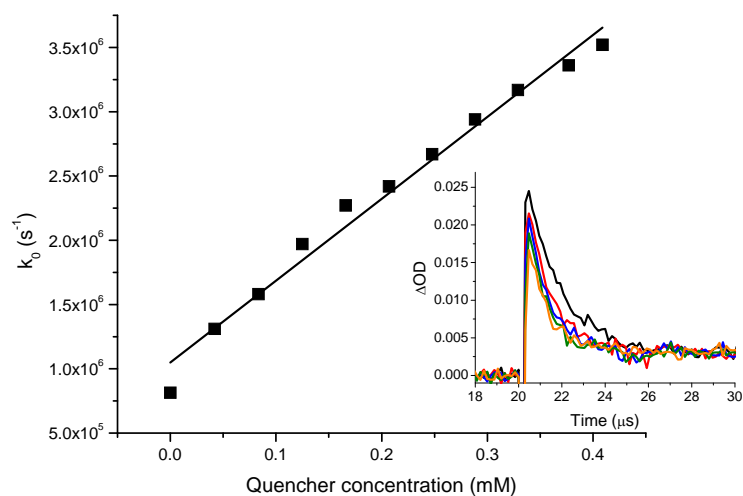


Figure S57. Quenching kinetics of **1** with 2-methylnaphthalene in acetonitrile. Inset: transient kinetics of **1** monitored at 420 nm as a function of 2-methylnaphthalene.

Laser flash photolysis of **2**

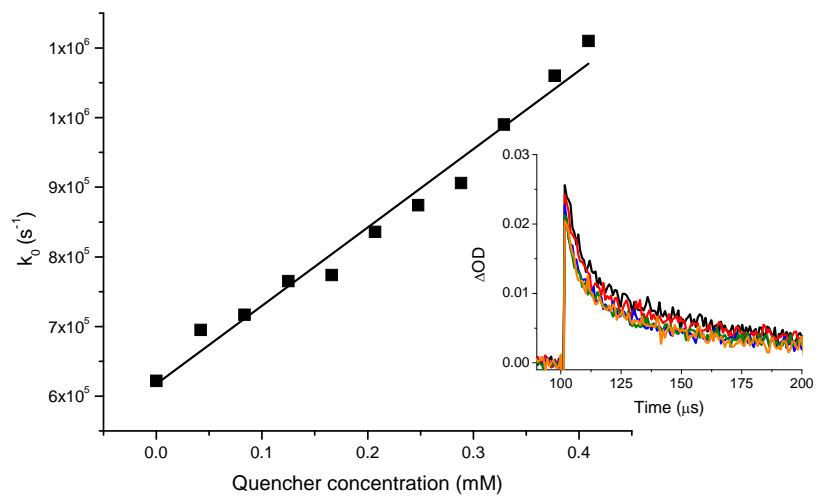


Figure S58. Quenching kinetics of **2** with 1,3-cyclohexadiene in acetonitrile. Inset: transient kinetics of **2** monitored at 420 nm as a function of 1,3-cyclohexadiene.

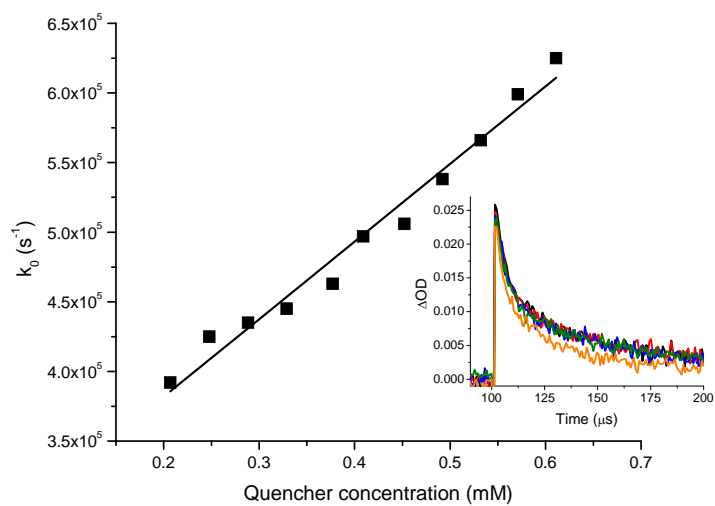


Figure S59. Quenching kinetics of **2** with 2-methylnaphthalene in acetonitrile. Inset: transient kinetics of **2** monitored at 420 nm as a function of 2-methylnaphthalene.

Laser flash photolysis of **3**.

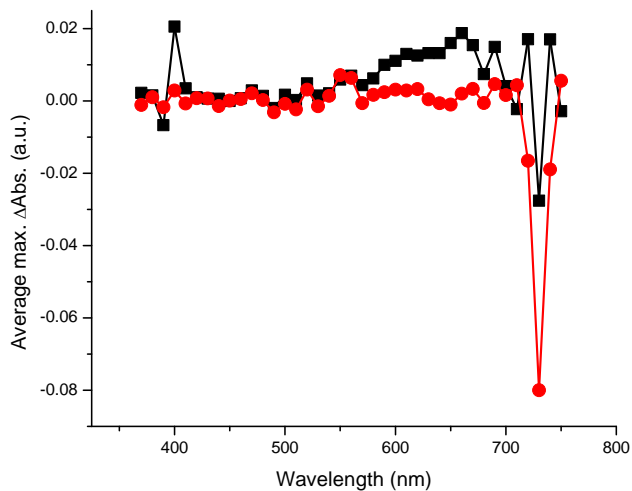


Figure S60. Transient absorbance spectra of **3** in acetonitrile upon excited at 355 nm.

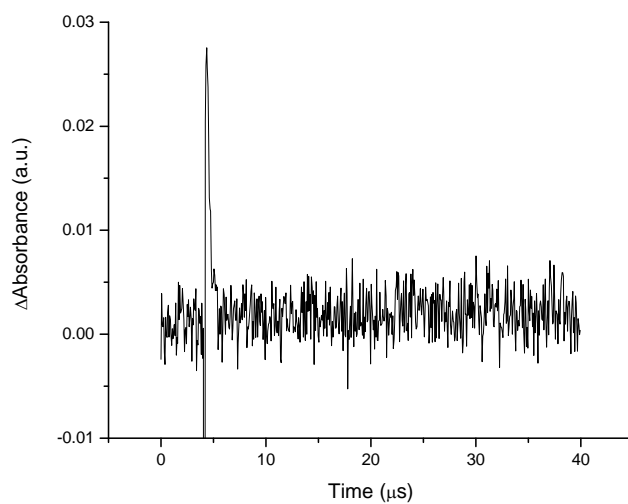


Figure S61. Transient absorbance kinetic of **3** monitored at 650 nm in acetonitrile.

Laser flash photolysis of **4**.

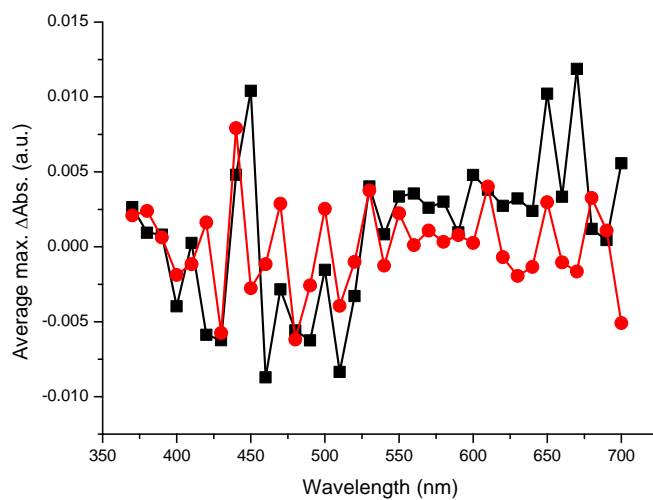


Figure S62. Transient absorbance spectra of **4** in acetonitrile upon excited at 355 nm.

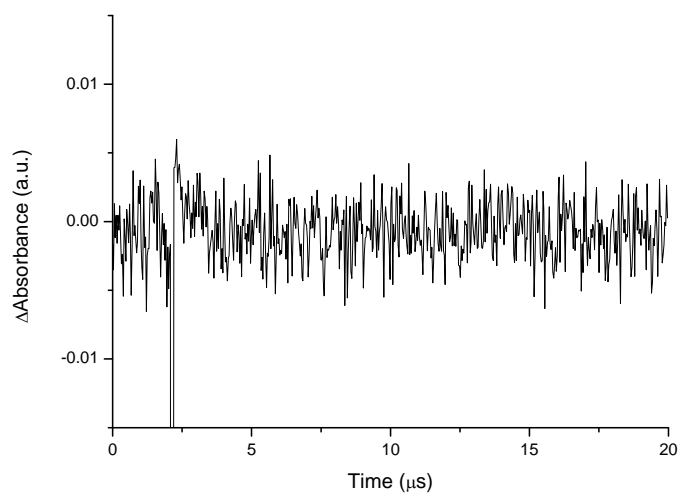


Figure S63. Transient absorbance kinetic of **4** monitored at 550 nm in acetonitrile.

Laser flash photolysis of **5**.

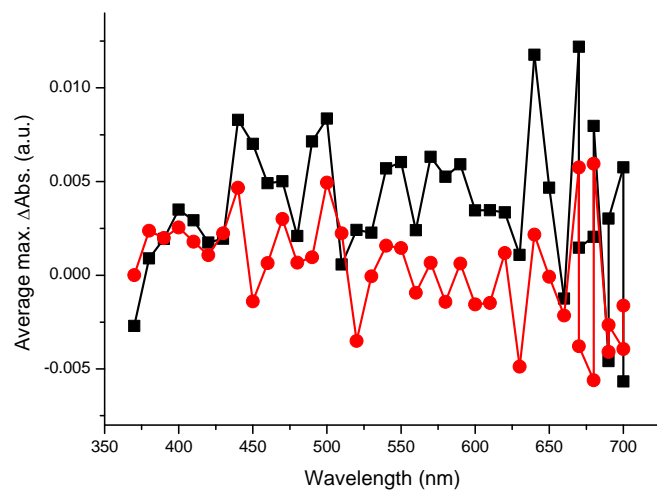


Figure S64. Transient absorbance spectra of **5** in acetonitrile upon exciting at 355 nm.

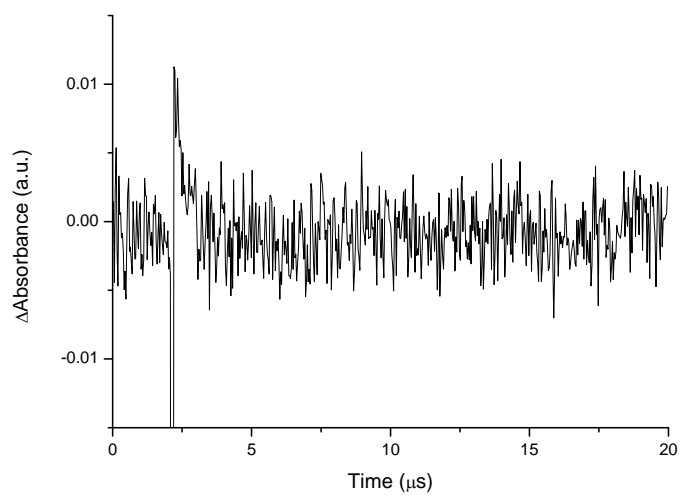


Figure S65. Transient absorbance kinetic of **5** monitored at 550 nm in acetonitrile.

Electrochemical properties.

Electrochemistry

The electrochemical properties of the compounds were investigated to complement the spectroscopic trends (*vide supra*). Of particular interest are the oxidation potentials given that thiophenes are known to be good hole transporting materials. The electrochemical studies further provide insight into the effect of the electronic groups on the HOMO and LUMO energy levels by examining the oxidation and reduction potentials, respectively. Taking **1** as the benchmark, the effect of both the nitro group and its placement on the bithiophene can be seen from the electrochemical data. As expected, the oxidation potential (E_{pa}) of **1** is the least positive of the series investigated owing its electron donating amine. The E_{pa} is increased by 100 mV for **2** relative to **1** (Table 2) as result of the electron withdrawing aldehyde that is conjugated with the amine. Replacing the aldehyde with the stronger electron withdrawing nitro group shifts the E_{pa} to values that are more positive by an additional 80 mV. Meanwhile the E_{pa} of **3** and **4** differ by only 30 mV. The higher E_{pa} of **4** vs. **3** is expected since the 4'-nitro is not conjugated with the amine, therefore it can exert its full withdrawing potential to increase the E_{pa} . This effect is further evident with **5** whose two nitro substituents work in concert to increase the oxidation potential. As seen in Figure 13, the oxidation processes for the aminothiophenes are quasi irreversible with the exception of **2** and **6**, whose oxidations are reversible. The lack of reversible oxidation for **1**, **3-5** is due to the generated radical cations that are highly reactive. The intermediates are understood to homocouple according to standard mechanisms, resulting in oligo- and polythiophenes.³⁷

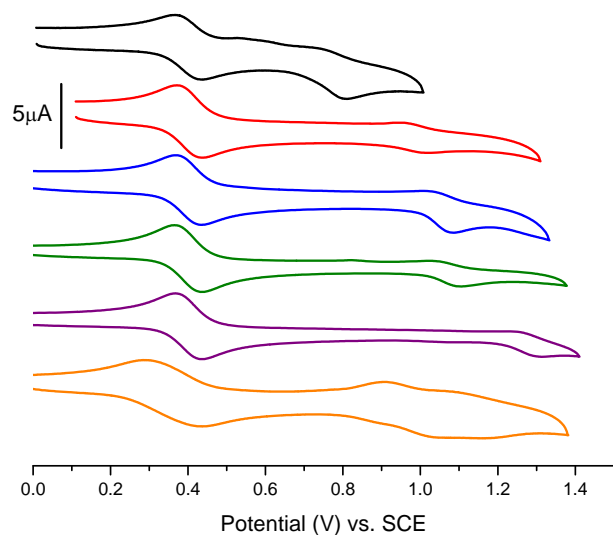


Figure S66. Cyclic voltammograms showing the anodic processes of **1** (—), **2** (—), **3** (—), **4** (—), **5** (—) and **6** (—) in deaerated dichloromethane with 0.1 M TBAPF₆ at 100 mV s⁻¹ with ferrocene as an internal reference (E_{pa} = 435 mV vs. SCE).

Electrochemical properties of **2**

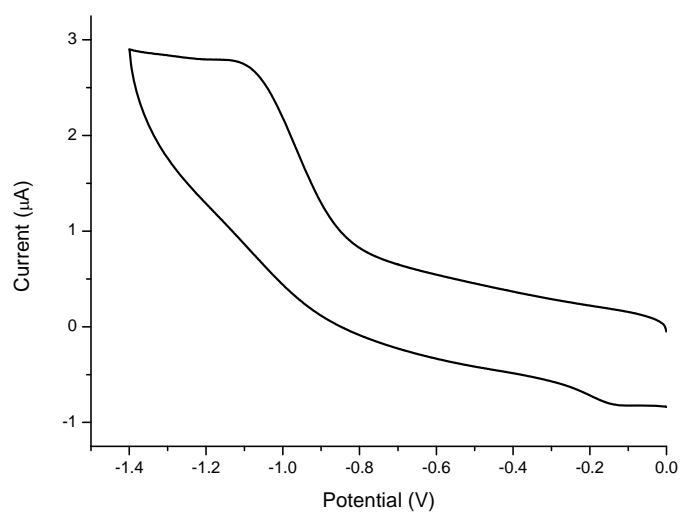


Figure S67. Cathodic cyclic voltammogram of **2** in dichloromethane with 0.1 M TBAPF₆ at 100 mVs⁻¹.

Electrochemical properties of **3**.

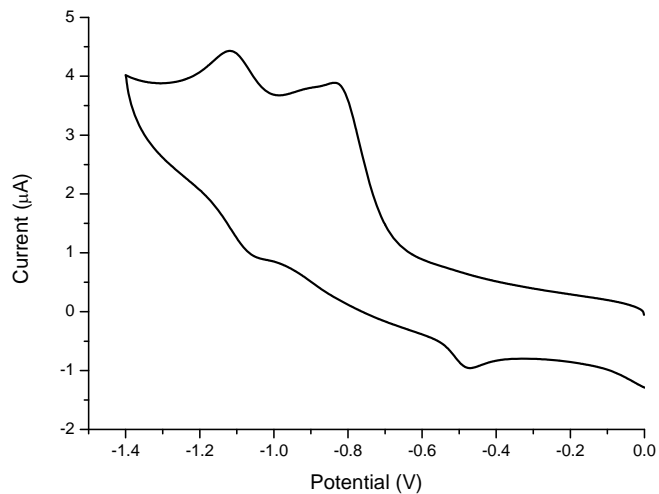


Figure S68. Cathodic cyclic voltammogram of **3** in dichloromethane with 0.1 M TBAPF₆ at 100 mVs⁻¹.

Electrochemical properties of **4**.

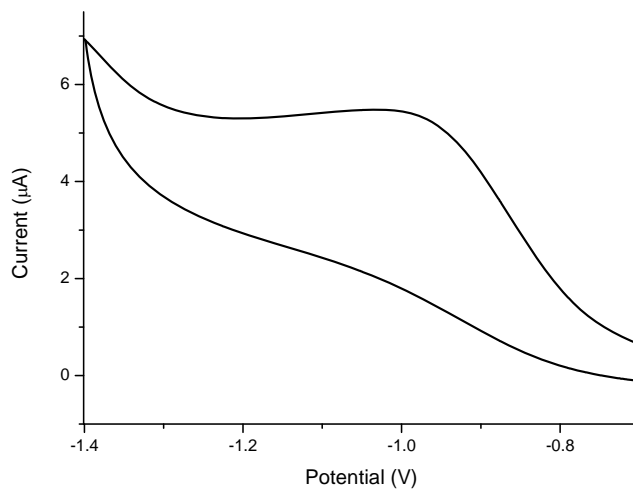


Figure S69. Cathodic cyclic voltammogram of **4** in dichloromethane with 0.1 M TBAPF₆ at 100 mVs⁻¹.

Electrochemical properties of **5**.

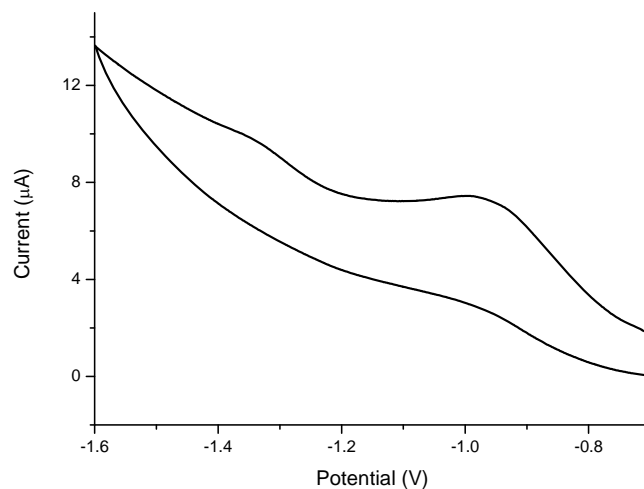


Figure S70. Cathodic cyclic voltammogram of **5** in dichloromethane with 0.1 M TBAPF₆ at 100 mVs⁻¹.

Electrochemical properties of **6**.

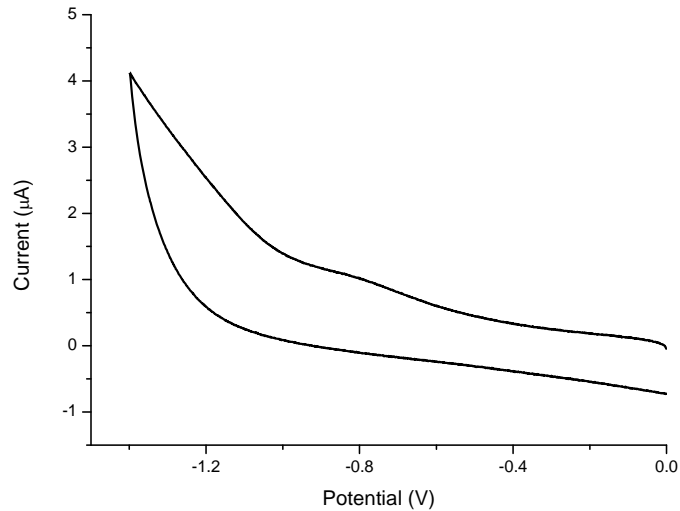


Figure S71. Cathodic cyclic voltammogram of **6** in dichloromethane with 0.1 M TBAPF₆ at 100 mVs⁻¹.